FRICKE RADIATION DOSIMETRY USING NUCLEAR MAGNETIC RESONANCE

by

Matthew B. Podgorsak
Department of Physics
McGill University, Montréal
November, 1989

A Thesis
submitted to the
Faculty of Graduate Studies and Research
in partial fulfillment of the
requirements for the degree
of Master of Science
in
Physics

ABSTRACT

The spin-lattice relaxation rate R_1 of irradiated Fricke solution was studied as a function of the absorbed dose D. The R_1 increases linearly with D up to a dose of ~250 Gy after which the response saturates. A model describing the R_1 of a solution of either ferrous (Fe^{2+}) or ferric (Fe^{3+}) ions is presented; it is based on fast exchange between protons on water molecules in the bulk and protons on water molecules in the coordination shell of the ions. All inherent relaxation parameters of the different proton groups are determined. An extension of the model is made to describe the spin-lattice relaxation behaviour of irradiated Fricke solution. Good agreement between model predictions and experimental results is observed. The model relates the spin-lattice relaxation rate of a Fricke dosimeter to the chemical yield of ferric ion, thus creating an absolute dosimetry technique. Various practical aspects of the NMR-Fricke system are described.

RÉSUMÉ

Le taux de relaxation spin-lattice R_1 d'une solution Fricke irradiée a été etudié en fonction de la dose absorbée D. R_1 augmente de façon linéaire avec D jusqu'à une dose ~250 Gy pour ensuite saturé. Un modèle décrivant R_1 d'une solution ionique ferreuse (Fe^{2+}) ou ferrique (Fe^{3+}) est presenté. Il est basé sur un échange rapide entre les protons des molécules d'eau non liées aux ions et les protons des molécules d'eau qui sont dans la couche de coordination ionique. Tous les paramètres de bases associés à la relaxation des différents groupes de protons sont determinés. Le modèle est developpé davantage pour décrire le comportement de la relaxation spin-lattice des solutions Fricke irradiées. Le modèle peut prédire très bien les résultats expérimentaux observés. Le modèle permet de relier le taux de relaxation spin-lattice de la méthode Fricke de dosimétrie au rendement chimique de l'ion ferrique, nous permettant ainsi de faire de la dosimétrie absolue. Plusieurs aspects pratiques des systèmes Fricke appliqués à la resonance magnétique nucléaire sont decrits.

ACKNOWLEDGEMENTS

The research described in this thesis has been performed under the auspices of the Department of Physics at McGill University, and has been carried out in the Departments of Medical Physics and Radiation Oncology situated at the Montreal General Hospital.

I am sincerely indebted to Dr. L. John Schreiner for his encouragement, support, direction, and undying patience during the course of this work. I also thank the various members of the Department of Medical Physics for their assistance. In particular, I would like to thank Mr. Lajos Palotay for suggesting, designing and constructing many of the mechanical apparatuses without which the effective use of the equipment could not be made. I also thank Mr. Joe Larkin for building the pulse programmer and for his numerous suggestions in trouble-shooting the electronics of the equipment. I thank Mr. Michael Evans, M.Sc. for helping with the TLD dose determination. Also appreciated are the many discussions I had with Professor E.B. Podgorsak as they clarified many concepts for me.

I also thank Dr. Ken R. Shortt at the National Research Council of Canada in Ottawa for supplying samples of Fricke solution and for the invaluable discussions we had. Especially appreciated is his critical review of the manuscript of this thesis. Many of his suggestions were incorporated into the final text.

I genuinely thank my family for their constant encouragement and support, especially during the times when I needed them most.

The financial assistance received from the Department of Physics through teaching assistantships and from the Natural Sciences and Engineering Research Council through grants-in-aid to Dr. L.J. Schreiner is acknowledged.

TABLE OF CONTENTS

LIST OF FIGURES

LIST OF TABLES

CHAPTER 1

BASIC THEORY

1.1 INTRODUCTION

In radiation therapy the primary goal is the destruction of malignant tissue with ionizing radiations (e.g., photons and electrons). The radiobiological effects of exposure to radiation are well understood and very specific protocols for treating different malignancies have been set. For an optimal response to radiotherapy it is essential that the actual radiation dose delivered to the treatment volume be within 5 percent of the dose prescribed by the particular protocol (ICRU, 1976). It becomes necessary, therefore, that the radiotherapy treatment units used to deliver the dose be calibrated and that the radiation dose actually delivered be well known.

Presently, there are a number of techniques in widespread use which allow one to calibrate a radiotherapy treatment unit. In most cases the calibration involves the use of ionization chambers or thermoluminescent materials. These two dosimetry tools are considered accurate within the required 5 percent, however, there are problems associated with both. The dosimeter, either an ionization chamber or a thermoluminescent material, is placed into a phantom which is irradiated. If the dosimeter material is not perfectly equivalent (density and atomic number) to the phantom material it will perturb the radiation field and the dose measured may not be equal to the

actual dose delivered in the absence of the dosimeter. Furthermore, determining the spatial distribution of dose to any reasonable resolution can be very tedious and labor-intensive. The thermoluminescent method has the added disadvantage that the analysis of the dosimeter causes the effective loss of the dose information.

As an alternative to the ionization chamber and thermoluminescent methods described above, chemical dosimetry has occasionally been used. Any well characterized and quantitative radiochemical reaction may serve as the basis for a dosimeter with the absorbed dose determined from a measurement of the progression of the radiation-induced reaction. The sensitivity of a chemical dosimeter is limited by the sensitivity of the probe used to quantify the chemical reaction. Early in the development of nuclear magnetic relaxation (NMR) it was observed that the spin-lattice and spin-spin relaxation times (T_1 and T_2, respectively) of certain materials decrease after irradiation (Abragam, 1961). It has therefore been suggested that NMR could be used to quantify the radio-chemical reaction (Gore et al., 1984). Typically, the probing of a chemical dosimeter is less sensitive than that of an ionization chamber or a thermoluminescent material. However, the ability to use NMR as a chemical dosimetry probe along with the advent of magnetic resonance imaging suggests the possibility for a direct measurement of dose in three dimensions. Thus, although the chemical dosimeter lacks the sensitivity of an ionization chamber, the three dimensional capability might compensate for the relative insensitivity.

The work presented in this thesis in an investigation of the use of proton NMR as a radiation dosimetry technique. In this chapter, the basic physics of NMR along with its application to radiation dosimetry will be discussed.

1.2 RELAXATION THEORY

1.2.1 Spin-lattice relaxation

The basic principles of NMR are reviewed in the literature. As a general overview, consider a sample of particles with spins in a static magnetic field $\mathbf{B}_o = B_o\hat{\mathbf{z}}$. Each particle has a magnetic moment $\mu = \gamma\hbar\mathbf{I}$, where γ is the gyromagnetic ratio and $\hbar\mathbf{I}$ is the nuclear spin angular momentum of the particle. The energy of a magnetic moment in a field $\mathbf{B}_o$ can be expressed classically as $E = -\mu\cdot\mathbf{B}_o$. Substitution of the quantum mechanical operator for μ leads to the semiclassical Hamiltonian of the system $\mathcal{H} = -\hbar\gamma B_o I_z$. The energy state of each nucleus is determined from the eigenstates of I_z. Each particle has a number of possible states whose Zeeman energies are given by $-m\gamma\hbar B_o$, where m is the magnetic quantum number and can have values of I_z, $I_z-1,\ldots,-I_z$. For example, spin 1/2 particles have magnetic quantum numbers $m = \pm 1/2$ hence there are two energy levels separated by $\gamma\hbar B_o$ and the resonant frequency, known as the Larmor frequency, is $\omega_o = \gamma B_o$. Each nucleus has a distinct value of γ, therefore, for a given magnetic field, various nuclei will resonate at different frequencies and one can limit observations exclusively to a particular nucleus. Since only proton relaxation will be

studied in this thesis, the following discussion, initially developed by Bloembergen et al. (1948) and Solomon (1955), will be restricted to spin 1/2 particles.

Any macroscopic sample contains an ensemble of weakly coupled spins which, when placed in the field $\mathbf{H}_o$, populate both Zeeman levels. The populations N_+ and N_- of the lower and upper Zeeman levels respectively are described in equilibrium by the Boltzmann distribution (Abragam, 1961):

$$\frac{N_+}{N_-} = \exp\left[\frac{\gamma\hbar H_o}{kT}\right] . \qquad (1.1)$$

At room temperature, $\gamma\hbar H_o \ll kT$ and, to a good approximation, the population ratio can be described as:

$$\frac{N_+}{N_-} = 1 + \frac{\gamma\hbar H_o}{kT} . \qquad (1.2)$$

Equation (1.2) shows that a greater number of spins are aligned with the magnetic field thereby producing a net equilibrium magnetization $\mathbf{M}_o$ along $\mathbf{H}_o$. The equilibrium magnetization may be altered in a number of ways. A redistribution of the population of the Zeeman energy states can be achieved by changing the magnitude of the applied magnetic field $\mathbf{H}_o$, or by applying a radio frequency (r.f.) field at the Larmor frequency either as a continuous irradiation or in short pulses. Following the perturbation, the spins relax toward the equilibrium distribution by exchanging energy with other spins and with the non-spin degrees of freedom in the surroundings, commonly refered to as the lattice.

In order to study the relaxation dynamics of a spin system, it is instructive to examine the quantum mechanical operators which describe the system. The Hamiltonian of a system of interacting particles of spin I_i in a magnetic field $\mathbf{H}_o = H_o\hat{\mathbf{z}}$ is:

$$\mathcal{H} = \mathcal{H}_M + \mathcal{H}_o + \mathcal{H}' , \tag{1.3}$$

where $\mathcal{H}_M$ is the Hamiltonian of the motion of the particles and commutes with the spin operators, $\mathcal{H}_o$ is the Zeeman Hamiltonian, and $\mathcal{H}'$ is a perturbation term due to the spin-spin interaction. For two particles of spins $\mathbf{I}$ and $\mathbf{S}$, the Zeeman Hamiltonian is:

$$\mathcal{H}_o = - \hbar\gamma_I H_o I_z - \hbar\gamma_S H_o S_z . \tag{1.4}$$

There are a number of spin-spin interactions which may contribute to spin-lattice relaxation: scalar coupling between magnetic moments, chemical shift anisotropy, quadrupolar and dipolar interactions, and the spin-rotation interaction. For protons on water molecules, however, scalar coupling, chemical shift anisotropy, and the quadrupolar interaction do not apply and the spin-rotation interaction is negligible (Schreiner, 1978). Thus, to a very good approximation, it can be assumed that the spin-spin interaction results from dipolar coupling and hence the perturbation term is (Solomon, 1955):

$$\mathcal{H}' = -\gamma_I\gamma_S\hbar^2\left[\frac{3(\mathbf{I}\cdot\mathbf{r})(\mathbf{S}\cdot\mathbf{r})}{r^5} - \frac{\mathbf{I}\cdot\mathbf{S}}{r^3}\right] , \tag{1.5}$$

where r is the distance between the spins.

The transition probability per unit time between two eigenstates $|m_i\rangle$ and $|m_j\rangle$ of the unperturbed Hamiltonian $\mathcal{H}_o$ is, to first order, given by the Fermi Golden Rule (Solomon, 1955):

$$w_{ij} = \frac{1}{t}\frac{1}{\hbar^2} \left| \int_o^t \langle m_j | \mathcal{H}'(t') | m_i \rangle e^{-i\omega_{ij}t'} dt' \right|^2, \qquad (1.6)$$

where $\omega_{ij} = (E_j - E_i)/\hbar$ with E_i and E_j the energies of the two eigenstates.

For particles of spin 1/2, the four eigenstates of the spins can symbolically be written as:

$$I_z|\pm\rangle = \pm \frac{1}{2} |\pm\rangle$$
$$S_z|\pm\rangle = \pm \frac{1}{2} |\pm\rangle. \qquad (1.7)$$

For a pair of spins, the four unperturbed eigenstates are $|+\rangle|+\rangle$, $|+\rangle|-\rangle$, $|-\rangle|+\rangle$, and $|-\rangle|-\rangle$ with respective populations of N_{++}, N_{+-}, N_{-+}, and N_{--}.

Figure 1 indicates the probabilities w_o, w_1, w_1', and w_2 for transitions between the four unperturbed eigenstates defined above. The time dependences of the population of each state with respect to the transition probabilities shown in Fig. 1 are:

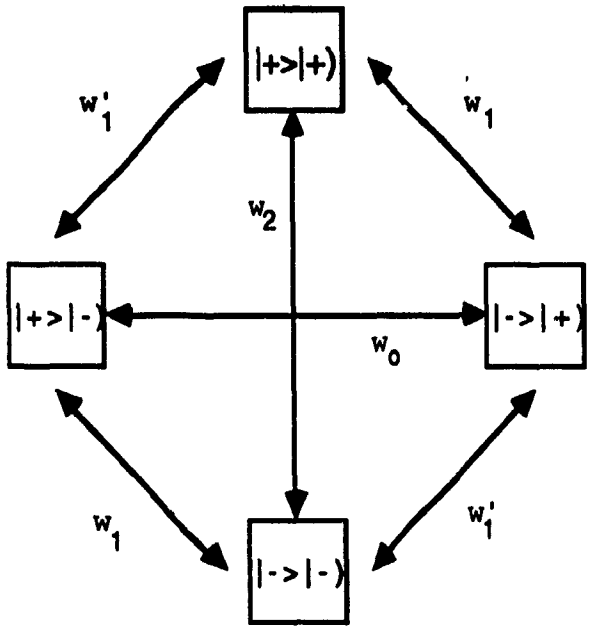

Figure 1 : Diagrammatic representation of the transition probabilities between the four unperturbed eigenstates |+>|+), |+>|-), |->|+), and |->|-) of a pair of identical spin 1/2 particles.

$$\frac{dN_{++}}{dt} = -(w_1+w_1'+w_2)N_{++} + w_1'N_{+-} + w_1N_{-+} + w_2N_{--} + \text{const.}$$

$$\frac{dN_{+-}}{dt} = w_1'N_{++} - (w_0+w_1+w_1')N_{+-} + w_0N_{-+} + w_1N_{--} + \text{const.}$$

$$\frac{dN_{-+}}{dt} = w_1N_{++} + w_0N_{+-} - (w_0+w_1+w_1')N_{-+} + w_1'N_{--} + \text{const.} \quad (1.8)$$

$$\frac{dN_{--}}{dt} = w_2N_{++} + w_1N_{+-} + w_1'N_{-+} - (w_1+w_1'+w_2)N_{--} + \text{const.}$$

In an NMR experiment, one observes the macroscopic magnetic moments $\langle I_z \rangle$ and $\langle S_z \rangle$ which have different Larmor frequencies and are related to the populations of the unperturbed eigenstates:

$$\langle I_z \rangle \propto (N_{++} + N_{+-}) - (N_{-+} + N_{--})$$
$$\langle S_z \rangle \propto (N_{++} + N_{-+}) - (N_{+-} + N_{--}) \; . \quad (1.9)$$

The equations of motion for the magnetic moments $\langle I_z \rangle$ and $\langle S_z \rangle$ are obtained by differentiating Eq. (1.9) and inserting the result into Eq. (1.8):

$$\frac{d\langle I_z \rangle}{dt} = -(w_o+2w_1+w_2)\langle I_z \rangle - (w_2-w_o)\langle S_z \rangle + \text{const}$$

$$\frac{d\langle S_z \rangle}{dt} = -(w_2-w_o)\langle I_z \rangle - (w_o+2w_1'+w_2)\langle S_z \rangle + \text{const}, \quad (1.10)$$

or,

$$\frac{d\langle I_z \rangle}{dt} = -(w_o+2w_1+w_2)[\langle I_z \rangle - I_o] - (w_2-w_o)[\langle S_z \rangle - S_o]$$

$$\frac{d\langle S_z \rangle}{dt} = -(w_2-w_o)[\langle I_z \rangle - I_o] - (w_o+2w_1'+w_2)[\langle S_z \rangle - S_o], \quad (1.11)$$

where I_o and S_o are the equilibrium values of the magnetic moments of spins **I** and **S**.

Equations (1.11) describe a decay which is, in general, a linear combination of two exponential functions. However, there are two cases which have solutions to Eq. (1.11) which are simple exponential functions:

(a) LIKE SPINS: If the two interacting spins are alike, they have the same gyromagnetic ratios, i.e., $\gamma_I = \gamma_S$. It is therefore only possible to observe the sum of the macroscopic magnetic moments $\langle I_z+S_z \rangle$ and, by definition, $w_1' = w_1$. Equation (1.11) then simplifies to:

$$\frac{d}{dt} \langle I_z+S_z \rangle = -2 (w_1+w_2) [\langle I_z+S_z \rangle - I_o - S_o]. \qquad (1.12)$$

The solution to Eq. (1.12) is a simple exponential function with a rate constant, termed the spin-lattice relaxation time, given by

$$\frac{1}{T_1} = 2(w_1+w_2). \qquad (1.13)$$

The transition probabilities can be computed with respect to the lattice dynamics. For example, Appendix 1 shows the calculation for the transition probabilities for two protons on a molecule assuming isotropic reorientation of the molecule. Substituting the calculated values of w_1 and w_2 into Eq. (1.13), the following equation for the spin-lattice relaxation time for a pair of like spins is obtained:

$$\frac{1}{T_1} = \frac{6}{20}\frac{\hbar^2\gamma^4}{r^6}\left[\frac{\tau_c}{1+\omega_o^2\tau_c^2} + \frac{4\tau_c}{1+4\omega_o^2\tau_c^2}\right], \qquad (1.14)$$

where $\omega_o = \gamma H_o$, the distance between the spins is r , and τ_c is the correlation time characteristic of the random motion of the water molecules. For isotropic reorientation, τ_c is considered to be the time for the water molecule to rotate 1 radian. Although Eq. (1.14) is specific to proton intramolecular relaxation due to a tumbling motion of the molecule, it has the general features that are obtained for other molecular motions.

(b) **RELAXATION IN A PARAMAGNETIC SOLUTION:** In most atoms, the magnetic moments produced by the orbital electrons cancel each other out, however, in the transition elements such as iron one or more of the inner electron orbitals is not filled resulting in a residual magnetic moment. When one of these atoms, known as paramagnetic atoms, is placed into a magnetic field, the time dependence of the large magnetic moment of the electron ($\gamma_S = 658\ \gamma_I$) dominates the spin-lattice relaxation.

The spin-lattice relaxation in a sample of pure water occurs primarily through the intramolecular and intermolecular dipole-dipole interaction between hydrogen nuclei in the same water molecule or in adjacent water molecules, respectively. When a paramagnetic ion is introduced into bulk water, the large local magnetic fields associated with the ion will dominate the local dipole-dipole interaction. To illustrate this effect consider the interaction between a hydrogen nucleus of spin I paired to the electronic spin S of a paramagnetic ion. The electron spin S itself does not relax very

efficiently through this dipole-dipcle interaction with I and to a good approximation, $S_z = S_o$, i.e., the electron spin state is constant. Then Eq. (1.11) reduces to:

$$\frac{d\langle I_z\rangle}{dt} = -(w_o+2w_1+w_2)\,[\langle I_z\rangle - I_o], \tag{1.15}$$

where the transition probabilities w_o , w_1, and w_2 are as defined previously. The solution to Eq. (1.15) is an exponential function with a relaxation time given by

$$\frac{1}{T_1} = w_o+2w_1+w_2 \ . \tag{1.16}$$

Substituting the values for the transition probabilities given in Appendix 1 leads to the following equation for the spin-lattice relaxation time in a paramagnetic solution:

$$\frac{1}{T_1} = \frac{1}{10}\frac{\hbar^2\gamma_I^2\gamma_S^2}{r^6}\left[\frac{\tau_c}{1+(\omega_I-\omega_S)^2\tau_c^2} + \frac{3\tau_c}{1+\omega_I^2\tau_c^2} + \frac{6\tau_c}{1+(\omega_I+\omega_S)^2\tau_c^2}\right], \tag{1.17}$$

where $\omega_I = \gamma_I H_o$, $\omega_S = \gamma_S H_o$, and τ_c is the correlation time of the random motion of the spins. Equation (1.17) describes the inherent spin-lattice relaxation for protons interacting with a paramagnetic center with spin S = 1/2. A more general form of the equation can be written for a paramagnetic center of arbitrary spin S (Solomon, 1955; Bloembergen and Morgan, 1961). In the notation used in this thesis,

$$\frac{1}{T_1} = \frac{2}{15}\frac{S(S+1)\hbar^2\gamma_I^2\gamma_S^2}{r^6}\left[\frac{\tau_c}{1+(\omega_I-\omega_S)^2\tau_c^2} + \frac{3\tau_c}{1+\omega_I^2\tau_c^2} + \frac{6\tau_c}{1+(\omega_I+\omega_S)^2\tau_c^2}\right]. \tag{1.18}$$

Equations (1.17 and 1.18) are based on a model which does not necessarily describe all paramagnetic solutions; it is derived for relaxation which is driven by an intramolecular interaction between two different spins on the same molecule. In most paramagnetic solutions, the dipole-dipole interaction occurs between spins on two different molecules, i.e., it is an intermolecular interaction between a hydrogen nucleus on a water molecule and an electron spin on a solvated ion. The relaxation time assuming an intermolecular dipole-dipole interaction, however, has the same form as Eq. (1.18) (Solomon, 1955). The correlation time τ_c is not simply a measure of molecular dynamics but it includes the combined time dependence from the molecular rotation and from the electron-spin relaxation (Gore et al., 1984). Bloembergen and Morgan (1961) include the contribution of a spin exchange interaction between the paramagnetic ions and the protons on the neighbouring water molecules, known as the contact hyperfine interaction, but for the ionic solutions studied in this thesis this term can be neglected (Bloembergen, 1956; Gore et al., 1984).

Only protons which are in the coordination shell of a paramagnetic ion will relax with a rate given by Eq. (1.18) (see Chapter 4). This is because the effect of the paramagnetic ion follows an r^{-6} dependence and decreases rapidly with increasing ion-proton distance. Thus in an ionic solution there exist two different types of water molecules: those in the hydration sphere of an ion (the so-called bound water) whose relaxation rate is given by Eq. (1.18) and those which are far from an ion (bulk water) and have relaxation rates identical to those of free water.

The potential of using NMR as a probe of irradiated Fricke solution is shown by Eq. (1.18). Irradiated Fricke solution contains two paramagnetic species with different spins and radii (see Chapter 4). Hence the measured proton relaxation rate of the solution depends on the relative quantity of each species which in turn depends on the dose absorbed by the Fricke solution.

1.2.2 Relaxation in heterogeneous spin systems

The theoretical analysis of the relaxation times shown above explains experimental data provided that the spin system is homogeneous. If, however, one is dealing with a heterogeneous spin system, such as an ionic solution, the apparent, i.e., observed spin-lattice relaxation may not be governed solely by the equations derived above. The spin relaxation in heterogeneous systems may be influenced by the exchange processes between different spin groups in the system. In most exchange models the exchange is considered to occur between two groups of spins and the coupled differential equations governing the evolution of the magnetizations for the two spin groups are solved (Edzes and Samulski, 1978; Schreiner et al., 1989). These models are especially applicable in the case of paramagnetic relaxation since water molecules outside the range of influence of the paramagnetic ion exchange with water molecules in the coordination shell of an ion by diffusion.

Figure 2 shows the spin lattice parameters for a system of two spin groups both with and without exchange. When exchange is present, the time dependence of the reduced magnetization of two spin groups is given by the coupled differential equations:

Figure 2 : The spin-lattice relaxation parameters for a system consisting of two spin groups a and b.

(a) No exchange present: the parameters shown are the inherent parameters; the relative sizes of the two spin groups are p_a and p_b and their respective relaxation rates are R_a and R_b. These inherent spin relaxation rates are determined by the molecular dynamics of the spin groups.

(b) Exchange present: the exchange rates are k_a and k_b . Both groups appear to relax with the rates λ^+ and λ^- and with magnetization fractions $p_a C_a^{\pm}$ and $p_b C_b^{\pm}$. The apparent spin relaxation rates are determined by the inherent spin relaxation rates and by the exchange rates between the two spin groups.

a)

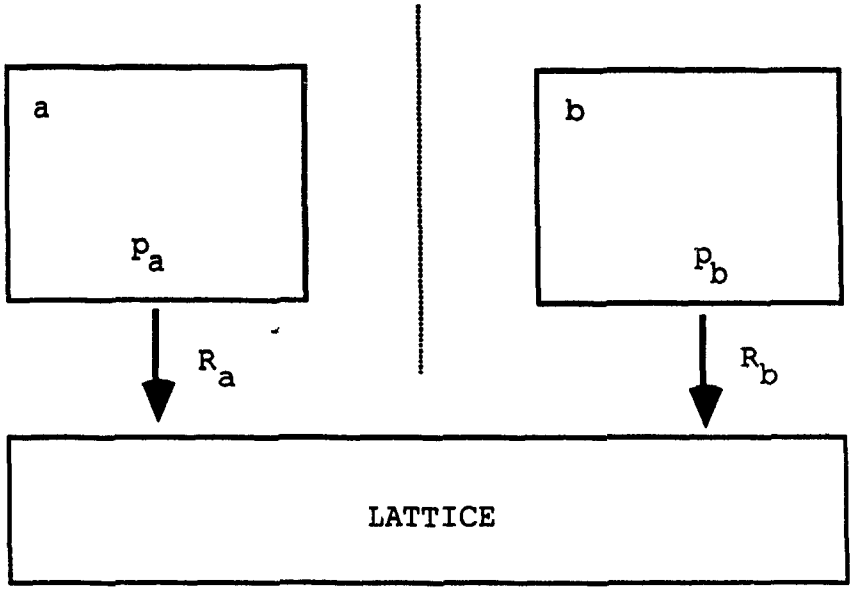
a
p_a
b
p_b
R_a
R_b
LATTICE

b)

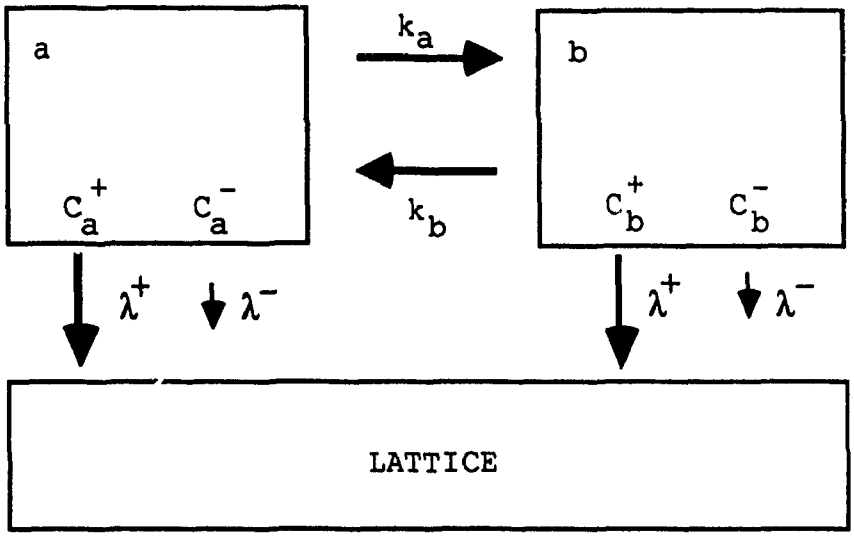
a
k_a
b
C_a^+
C_a^-
k_b
C_b^+
C_b^-
λ^+
λ^-
λ^+
λ^-
LATTICE

$$\frac{d\,\delta M_a}{dt} = - R_a\,\delta M_a - k_a\,\delta M_a + k_a\,\delta M_b \qquad (1.19a)$$

$$\frac{d\,\delta M_b}{dt} = - R_b\,\delta M_b - k_b\,\delta M_b + k_b\,\delta M_a, \qquad (1.19b)$$

where R_a and R_b are the inherent relaxation rates of the respective spin groups given by Eqs. (1.14 and 1.18). The inherent rates are the rates with which each spin group would relax if there were no coupling, i.e., if relaxation were determined by the dynamics of each group alone. The exchange constants k_a and k_b couple the magnetization evolution of the two groups. The coupling could result, for example, from exchange of protons between different spin groups (e.g. diffusion of water molecules between groups) or from exchange of magnetization through spin-spin interactions (Schreiner et al., 1989). The reduced magnetizations δM_a and δM_b for T_1 inversion recovery measurements (see Chapter 3) are defined by:

$$\delta M = \frac{M_\infty - M_z(\tau)}{2\,M_\infty} . \qquad (1.20)$$

The solutions of Eqs. (1.19) are (Zimmerman and Brittin, 1957):

$$\delta M_a(\tau) = C_a^+ e^{-\lambda^+\tau} + C_a^- e^{-\lambda^-\tau} \qquad (1.21)$$

$$\delta M_b(\tau) = C_b^+ e^{-\lambda^+\tau} + C_b^- e^{-\lambda^-\tau} . \qquad (1.22)$$

The magnetizations of each of the two spin groups relax as the sum of two exponentials with the apparent relaxation rates λ^- and λ^+ given by:

$$\lambda^{\pm} = \frac{1}{2} \{(R_a + R_b + k_a + k_b) \pm [(R_a - R_b + k_a - k_b)^2 + 4\, k_a k_b]^{1/2}\}. \quad (1.23)$$

The $C_a^{\pm}$ and $C_b^{\pm}$ are the apparent magnetization fractions of the magnetization evolution defined by Eqs. (1.21-1.22). They are also functions of the inherent relaxation rates and the exchange rates (Zimmerman and Brittin, 1957; Schreiner et al., 1989).

The apparent relaxation rates are complex functions of the exchange rates k_a and k_b as well as the inherent relaxation rates R_a and R_b. The effect of exchange on the apparent relaxation rates depends upon the magnitude of the exchange rates relative to the inherent relaxation rates. Three regimes of exchange can be identified: slow, intermediate, and fast exchange. In slow exchange, the exchange rates are much smaller than the inherent relaxation rates and the relaxation can be modelled by spin dynamics alone, i.e., the apparent relaxation rates are the inherent rates ($\lambda^+ = R_a$ and $\lambda^- = R_b$). A system which is in intermediate exchange, i.e., with exchange rates comparable to the inherent relaxation rates, relaxes with rates given by Eq. (1.23). In fast exchange, however, the exchange rates are much larger than the inherent relaxation rates (k_a, $k_b \gg R_a$, R_b) and the relaxation of the system becomes mono-exponential with a characteristic relaxation rate which is the weighted average of the inherent rates (Zimmerman and Brittin, 1957; Schreiner and Podgorsak, 1989), i.e.,

$$\delta M(\tau) = C^- e^{-\lambda^- \tau}, \quad (1.24)$$

with

$$\lambda^- = p_a R_a + p_b R_b . \quad (1.25)$$

1.2.3 Spin-spin relaxation

As mentioned previously, a spin which is in an excited state relaxes toward equilibrium through interactions within the spin system and between the spin system itself and its surroundings. The interaction between the spins themselves, called spin-spin relaxation, can also be probed. Spin-spin relaxation was not studied in this thesis, however, and the reader is referred to the literature (e.g. Slichter, 1978) for a further discussion of spin-spin relaxation.

CHAPTER 2

CHEMICAL DOSIMETRY

2.1 INTRODUCTION

Chemical dosimetry is based on the chemical change which may occur in a material being irradiated. The material, known as the dosimeter, can be a solid, gas, or liquid. The most widely characterized chemical dosimeters are aqueous solutions; solid and gas dosimeters have been studied but to a lesser extent (ICRU, 1961).

As was mentioned in §1.1, a major problem in accurately determining dose is the fact that the dosimeter may perturb the radiation field in the material in which one is trying to determine the dose. Therefore, to obtain an accurate measure of the dose at a point in a phantom, it is desirable to have a dosimeter which does not differ significantly from the medium in question, i.e., the dosimeter must have approximately the same density and atomic composition as the phantom. Chemical dosimeters are especially useful since they offer a very broad range of flexibility in terms of density and atomic composition.

A dosimeter based on chemical reactions which occur in aqueous solutions is comprised of a reaction cell, usually made of quartz, glass or polyethylene, inside of which is the aqueous solution which is chemically altered as a result of exposure to radiation. The reaction cell wall will have no effect on the radiolytic reactions if the dosimeter solution is in electronic

equilibrium with the surroundings or if the physical dimensions of the cell are large compared with the range of secondary electrons created both in the cell wall and in the dosimeter solution. According to the Bragg-Gray Cavity theory (Johns and Cunningham, 1983), in electronic equilibrium there is no net energy transfer between electrons created in the cell wall and in the solution itself. If the cell is irradiated in air but its wall is too thin, i.e., small compared to the range of the secondary electrons generated in the wall material, the chemical yield of the dosimeter solution may be altered (Weiss, 1952). If, however, irradiations are performed in phantom, then electronic equilibrium is assured and in order to minimally perturb the radiation field in the phantom either a very thin cell wall or a wall material equivalent to the phantom is desired.

It is possible to measure doses between 0.1 and 10^8 Gy using chemical dosimetry, however no single dosimeter will reliably cover this range (Attix et al., 1966). Since the sensitivity of dosimeters varies it is necessary to account for the order of magnitude of the dose to be measured. Another requirement of chemical dosimetry is a reasonable stability of the dosimeter both before and after irradiation in order to obtain reproducible dose measurements. Variables which should not become factors in chemical dosimetry are the dose rate, quality of the radiation, and temperature. Also, the preparation of the dosimeter should be simple and extensive purification of its constituents should not be necessary.

One dosimeter which meets most of the above requirements was developed about 60 years ago by Fricke and Morse (1927). The Fricke

dosimeter is based on the oxidation of an aerated ferrous sulfate solution and is readily reproducible. Dose measurements with the Fricke technique have been calibrated through intercomparisons with water and graphite calorimetry (Mosse et al., 1982; Ross et al., 1989). The main drawbacks of the Fricke dosimeter are a limited measurable dose range because of the relative insensitivity of the spectrophotometric analysis method, and a dose rate dependence at very high dose rates (Miller, 1953).

2.2 BASIC PRINCIPLES

2.2.1 The basis of radiolytic reactions

The detailed theory of the processes which occur when radiation interacts with a chemical dosimeter has been reviewed extensively (Allen, 1961; Hart and Platzman, 1961; Spinks and Woods, 1964). In this section, a brief introduction to the physical and chemical basis of the radiochemical reactions which occur in aqueous solutions is presented.

In dilute aqueous systems the interactions between water molecules and radiation result in the production of free radicals and molecular products. The initial interactions produce the ions HOH^+ and HOH^-, and hydrated electrons via the following reactions:

$$H_2O \rightarrow HOH^+ + e^- \qquad (2.1)$$

$$H_2O + e^- \rightarrow HOH^- \qquad (2.2)$$

$$e^- + n\, H_2O \rightarrow e_{aq}^- , \qquad (2.3)$$

where η designates that the electron is hydrated by water molecules. The two ions quickly dissociate to form the free radicals H• and •OH:

$$HOH^+ \rightarrow H^+ + \bullet OH \qquad (2.4)$$

$$HOH^- \rightarrow OH^- + H\bullet . \qquad (2.5)$$

These free radicals may combine to form other chemical species:

$$H\bullet + H\bullet \rightarrow H_2 \qquad (2.6)$$

$$\bullet OH + \bullet OH \rightarrow H_2O_2 . \qquad (2.7)$$

The interaction of radiation with water thus produces a free radical group comprised of hydrogen (H•) and hydroxyl radicals (•OH) and hydrated electrons (e_{aq}^-) in addition to the molecular products hydrogen (H_2) and hydrogen peroxide (H_2O_2). At low pH, the e_{aq}^- is quickly converted to H• by the reaction

$$e_{aq}^- + H^+ \rightarrow H\bullet , \qquad (2.8)$$

however, at high pH, the e_{aq}^- is stable enough that it can react with dissolved substances or with water molecules in the following reaction:

$$e_{aq}^- + H_2O \rightarrow H\bullet + OH^- . \qquad (2.9)$$

This explains the pH dependency of most radiolytic reactions. In addition to reactions (2.8) and (2.9), the following reactions occur:

$$e_{aq}^- + e_{aq}^- (+ 2\ H_2O) \rightarrow H_2 + 2\ OH^- \quad (2.10)$$

$$e_{aq}^- + \cdot OH \rightarrow OH^- \quad (2.11)$$

$$e_{aq}^- + H\cdot\ (+H_2O) \rightarrow H_2 + OH^- \quad (2.12)$$

$$H\cdot + \cdot OH \rightarrow H_2O\ . \quad (2.13)$$

The free radical and molecular product yields are usually expressed in terms of the quantity of molecules or radicals formed per 100 eV of absorbed energy and are designated by the letter G subscripted with the appropriate product. Table 1 (Barr and Schuler, 1957) lists the measured chemical yields for the species formed as a result of the interaction of radiation with water. (The value of the chemical yield in SI units (M/Gy) can be obtained by using the conversion: 1 ion/100 eV = 1.04×10^{-7} M/Gy.) The effect of pH is demonstrated by the difference in the G values for Co-60 gamma rays interacting with water and a 0.8 N H_2SO_4 solution.

2.2.2 Calculation of dose

Most chemical reactions which are radiation induced can be represented as follows:

$$\mathbf{A} + \mathbf{B} \rightarrow \mathbf{C} + \mathbf{X}. \quad (2.14)$$

The dosimeter solution itself is comprised of a species **A** which reacts with species **B** generated by irradiation to give products of which at least one, say **X**, can be quantitatively studied. As stated above, the amount of **X** produced as a result of the radiation exposure is known as G(X). When the reaction proceeds in a dose range where

Radiation	Solution	$G_{H\cdot}$	$G_{\cdot OH}$	G_{H_2}	$G_{H_2O_2}$	$G_{e^-_{aq}}$
$Co^{60}\gamma$ rays	0.8 N H_2SO_4	3.70	2.92	0.39	0.78	0
$Co^{60}\gamma$ rays	H_2O	0.55	2.20	0.45	0.70	2.85

Table 1 : Radiation yields (in molecules or radicals formed per 100 eV of absorbed energy) in aerated aqueous solutions (Barr and Schuler, 1957). The chemical yields can be calculated in SI units using the conversion factor: 1 ion/100 eV = 1.04×10^{-7} M/Gy.

the amount of product is linear with respect to dose, the yield is obtained from

$$G(X) = 100 \frac{\Delta n}{\Delta E} , \qquad (2.15a)$$

where Δn is the number of molecules of X formed per unit volume of dosimeter solution and ΔE is the energy in eV absorbed by the dosimeter per unit volume. There are many different methods used to determine Δn and, in fact, one goal of this thesis is to investigate the use of NMR to determine Δn. The energy absorbed by the dosimeter is determined by other dosimetry techniques such as calorimetry, thermoluminescence, or ionization. Attix et al. (1966) give a more complete discussion of these methods.

Once the chemical yield for a particular reaction is known, the absorbed energy per unit volume, which is proportional to the dose absorbed by the medium, is obtained from Eq. (2.15a):

$$\Delta E = 100 \frac{\Delta n}{G(X)} . \qquad (2.15b)$$

If the amount of X produced as a result of the irradiation is expressed as a change in concentration ΔM, the dose D in Gy is given by:

$$D = 9.64 \times 10^{9} \frac{\Delta M}{G(X)\, \rho} , \qquad (2.16)$$

where ΔM is in moles/liter (M), ρ is the density of the aqueous dosimeter solution in kg/m^3, G(X) has units of ions or radicals

formed per 100 eV of absorbed energy and the constant 9.64×10^9 incorporates the conversions : 1 Gy = 1 J/kg and 1 eV = 1.602×10^{-19} J.

Equation (2.14) is general for chemical reactions with linear dose responses and can be used once the chemical yield for a particular reaction is determined.

2.3 FRICKE FERROUS SULFATE DOSIMETER

2.3.1 Standard Fricke dosimeter

The use of ferrous sulfate as a chemical dosimeter was first proposed by Fricke and Morse (1927). It has become the most reliable and most widely used chemical dosimeter. Fricke dosimetry is based on the oxidation of ferrous (Fe^{2+}) ion to ferric (Fe^{3+}) ion which occurs as a result of exposure of a solution of aqueous ferrous ions to radiation.

The standard ferrous sulfate dosimeter, known as Fricke solution, is comprised of 1 mM ferrous ions, obtained from aqueous ferrous ammonium sulfate [$Fe(NH_4)_2(SO_4)_2$] or aqueous ferrous sulfate [$FeSO_4$], and 0.8 N H_2SO_4. These concentrations were initially chosen to provide the same mass absorption coefficient for x rays in the ferrous sulfate solution as in air (Fricke and Petersen, 1927).

The oxidation of the ferrous ions to ferric ions proceeds in three stages:

(1) **The physical stage:** This stage comprises the bulk of the primary interactions of the solution with the incident radiation. Since the system does not have a very high concentration of solute, most of the initial interactions are between the incident radiation and the solvent water. These interactions occur within 10^{-8} seconds (Dyne and Kennedy, 1958) and result in the production of ionized and excited species along with secondary electrons.

(2) **The physico-chemical stage:** Before any ionic or molecular diffusion in the system has occured, the products formed in the physical stage rearrange and react with each other. Within 10^{-11} seconds of the previous stage, the secondary electrons are hydrated and thermalized, i.e., they lose their energy through collisions with the medium. Hence, in the first two stages, reactions (2.1-2.3) have occured.

(3) **The chemical stage:** As the primary species diffuse away from their point of origin, the chemical stage commences and the primary species react with solute species in the solution. At low pH, the first reaction to occur is reaction (2.8) followed, in an aerated system, by

$$H\bullet + O_2 \rightarrow HO_2\bullet \ . \qquad (2.17)$$

The oxidation of ferrous to ferric ion occurs according to the following reactions:

$$\bullet OH + Fe^{2+} \rightarrow Fe^{3+} + OH^- \qquad (2.18)$$

$$HO_2\bullet + Fe^{2+} \rightarrow Fe^{3+} + HO_2^- \qquad (2.19)$$

$$HO_2^- + H^+ \rightarrow H_2O_2 \qquad (2.20)$$

$$H_2O_2 + 2\ Fe^{2+} \rightarrow 2\ Fe^{3+} + 2\ OH^-. \qquad (2.21)$$

In summary, each hydrogen radical forms one hydroperoxy radical ($HO_2\bullet$) and each hydroperoxy radical oxidizes three ferrous ions: one directly by reaction (2.19) and two indirectly by reactions (2.19), (2.20), and (2.21). One ferrous ion is also oxidized by a hydroxyl radical ($\bullet OH$) through reaction (2.18) and two more ferrous ions are oxidized by one hydrogen peroxide molecule (H_2O_2) through reaction (2.21). It is therefore possible to write the chemical yield of ferric ion as (Attix et al., 1966)

$$G(Fe^{3+}) = 2\ G(H_2O_2) + 3\ G(H\bullet) + G(\bullet OH), \qquad (2.22)$$

where the yields for the hydrogen peroxide molecule, $G(H_2O_2)$, hydrogen atom, $G(\bullet H)$, and hydroxyl radical, $G(\bullet OH)$, are given in Table 1. Using these values and Eq. (2.22), the chemical yield of ferric ion is 15.5 ions per 100 eV (or, in SI units, $G(Fe^{3+})$ is 1.61×10^{-6} M/Gy).

Reaction (2.17) involves the consumption of oxygen, therefore standard Fricke solutions must be aerated. Once all the dissolved oxygen in the system has been consumed, reaction (2.17) can no longer proceed and the hydrogen radical which would normally form a hydroperoxy radical that would oxidize three ferrous ions instead oxidizes only one ferrous ion:

$$H\bullet + Fe^{2+} + H^+ \rightarrow Fe^{3+} + H_2. \qquad (2.23)$$

The chemical yield of the ferric ion is then

$$G(Fe^{3+}) = 2\ G(H_2O_2) + G(H\bullet) + G(\bullet OH), \qquad (2.24)$$

which gives a value of 8.2 ions per 100 eV (8.53×10^{-7} M/Gy). This property of the Fricke solution implies that once all the dissolved oxygen in the system has been consumed, the response of the dosimeter will change, hence an upper dose limit for accurate measurement is usually quoted as 400 Gy for Fricke solutions made with an initial ferrous ion concentration of 1 mM (Ellis, 1974). Reaction (2.17) does not abruptly cease at some dose, however, so the upper dose limit is in practical terms lower than 400 Gy.

2.3.2 Modified Fricke dosimeter

The chemical yields which have been quoted in the previous section are for aqueous solutions which are free of any impurities. Dewhurst (1952) noted that very small concentrations of organic impurities can greatly increase the chemical yields of the ferric ion, while phenols (Ahrens, 1967) and organic sulfides (Jayson and Wilbraham, 1968) inhibit the oxidation of the ferrous ion thus causing a decrease in the yield. Hence, if the Fricke solution is not entirely free of impurities, the chemical yield of the solution will differ from that determined from Eq. (2.22).

In the presence of organic impurites (such as alcohols (Dewhurst, 1952), unsaturated hydrocarbons (Basson and Du Plessis, 1967), and carboxylic acids (Hart, 1955)) the organic radical

competes with the ferrous ion for reaction with the hydroxyl radical •OH. Then, in addition to reactions (2.17 - 2.21), the following reaction chain can occur:

$$\bullet OH + RH \rightarrow R\bullet + H_2O \qquad (2.25)$$

$$R\bullet + O_2 \rightarrow RO_2\bullet \qquad (2.26)$$

$$RO_2\bullet + Fe^{2+} + H^+ \rightarrow RO_2H + Fe^{3+} \qquad (2.27)$$

$$RO_2H + Fe^{2+} \rightarrow Fe^{3+} + RO + OH^- , \qquad (2.28)$$

where R• represents the organic radical. Reaction (2.25) competes with reaction (2.18), and this chain of reactions can increase the chemical yield of the ferric ion by up to a factor of two in the presence of relatively high concentrations of organic impurities.

In order to protect the system from high chemical yields resulting from trace organic impurities, sodium chloride is added to the standard Fricke solution. The modified Fricke dosimeter is comprised of standard Fricke solution together with 1 mM NaCl and it is this modified solution which is usually used. In the presence of chloride ion, the hydroxyl radical in reaction (2.25) reacts with the chloride ion more readily than with the organic impurity. Therefore, reaction (2.25) is replaced by

$$\bullet OH + Cl^- \rightarrow Cl\bullet + OH^- , \qquad (2.29)$$

and only one Fe^{3+} is formed per hydroxyl radical:

$$Fe^{2+} + Cl\bullet \rightarrow Fe^{3+} + Cl^-, \qquad (2.30)$$

as is the case in uncontaminated Fricke solution. Because competitive reactions occur, the protective effect of NaCl is not complete and, in practice, the amount of desensitization depends on the type and relative concentration of impurity.

A good test to determine if the system is in fact free of impurities has been proposed by Fricke and Hart (1966). It involves the determination of the chemical yields both in the presence and absence of NaCl. If the yields are equal within experimental error, then the system is assumed to be adequately pure. This technique assumes that changes in the reaction mechanism occur only in the presence of impurities, and that sodium chloride has no effect on a pure system. Cottens et al. (1982) have shown that this assumption is not entirely true, and that the chloride ion does have an effect on $G(Fe^{3+})$ which is not related to the suppression of impurity effects. They found that the addition of sodium chloride decreases the chemical yield of ferric ion even in the absence of impurities. This is attributed to an initial decrease in H_2O_2 production, due to the chloride ion, during the diffusion of the radiolytic species from their site of origin. A cubic root relationship between $G(Fe^{3+})$ and the concentration of Cl^- was found. However, at a sodium chloride concentration of 1 mM, the drop in chemical yield is only 0.5 percent. Therefore, if the chemical yield of ferric ion in the presence of sodium chloride is within 0.5 percent of the yield for the standard Fricke solution, the system is considered to be free of impurities.

2.4 REVIEW OF THE DEVELOPMENT OF NMR DOSIMETRY

Chemical dosimetry has been in use for many years, however, it was not until 1984 that Gore et al. introduced the possibility of using NMR to monitor the progression of a radio-chemical reaction. As described above, the radiation chemistry of the Fricke ferrous sulfate dosimeter can be summarized as the conversion of the ferrous ion, Fe^{2+}, to the ferric ion, Fe^{3+}. For a large dose range the ferric ion concentration in the Fricke solution increases linearly with dose. Conventionally the concentration of ferric ion is measured spectrophotometrically. Gore et al. (1984) realized that since the two paramagnetic ions Fe^{2+} and Fe^{3+} have different paramagnetic spin states and ionic radii, they have different enhancing effects on the proton relaxation of aqueous Fricke solution. Therefore the irradiated Fricke solutions should have a dose dependent spin relaxation behavior. Using a high power solid state NMR spectrometer and small samples of Fricke solution, Gore et al. (1984) observed a linear increase in the spin-lattice and spin-spin relaxation rates (T_1^{-1} and T_2^{-1}) of the solutions with dose. The slope relating the spin-lattice relaxation rate change to the absorbed dose, in this thesis called the NMR sensitivity to radiation, was 0.0113 s^{-1} Gy^{-1} in the absorbed dose interval 0 to 50 Gy. The sensitivity was slightly different than that expected from the established chemical yield of ferric ion. This difference was attributed to experimental error. Gore et al. (1984) noted that, as usual for chemical dosimetry, the technique was somewhat insensitive to low doses but that it did have the advantage that sample sizes

could be very small and that the imaging modality of NMR could be a further asset in NMR dosimetry. To illustrate this they imaged a phantom containing five sample tubes with solutions which had been irradiated in the range from 0 to 41 Gy. There was a clear variation in the image intensity of the different tubes, however, no attempt to correlate the image intensity with the dose was made. More recently the group has been developing gel phantoms infused with Fricke solutions to use with MRI dosimetry (deGuzman et al., 1989). The goal is to limit the diffusion of the Fricke solution throughout the phantom thereby ensuring spatial stability of the dose distribution measurements.

The first group to report the development of practical MRI dosimeters was Hiraoka et al. (1986) in Japan. They developed a tissue equivalent phantom containing a Fricke solution fixed in a cross-linked dextran gel. After irradiating the phantom to doses up to 50 Gy under varying conditions, the change in the spin-lattice relaxation rate of the phantom, as measured with a magnetic resonance imager, was compared to the rate change in the Fricke solution alone. It was noted that the NMR sensitivity to radiation was higher in the gel system than in the corresponding aqueous Fricke solution. Also, the change in the spin-lattice relaxation rate was linear in the whole range for the aqueous Fricke solution, however, the gel fixed solutions showed a linear dose response to 35 Gy only; at higher doses the response was saturated. Appleby et al. (1987, 1988) have proposed a mechanism to explain the increased dose sensitivity in the gel dosimeters. Essentially the gel acts as an organic impurity and contributes additional radio-chemical pathways thereby increasing the yield of ferric ion. Appleby et al. (1987, 1988) have also

irradiated an agarose gel Fricke solution phantom and they report a 1 mm resolution in a 3-dimensional NMR dose determination. The sensitivity of the technique was increased by incorporating benzoic acid into the Fricke solution. Rather than report relaxation times, they gave their results in terms of the optical density of films taken of the inversion recovery MR image. The image brightness varied linearly with dose up to 11 Gy at which point the dose response saturated.

Szeredi et al. (1986) have also investigated aqueous and gel-fixed Fricke dosimeters with both NMR and MRI. For the aqueous dosimeters they observed an NMR sensitivity to dose for the spin-lattice relaxation rate of 0.018 $s^{-1}Gy^{-1}$, about 60 % higher than that reported by Gore et al. (1984). This result has been reproduced by the Swedish group of Olsson et al. (1988, 1989) using an NMR spectrometer. Neither group has given any explanation for the increased NMR sensitivity to radiation for their aqueous Fricke solutions, as compared with the published work of Gore et al. (1984). In 1986, Scielzo et al. found a linear dose response in the signal intensity of irradiated Fricke solution as measured with an inversion recovery pulse sequence with an MR scanner. The dose range investigated was 0 to 20 Gy. The sensitivity of their solution to radiation was not published.

To date there have been a few publications, described above, which qualitatively describe the measurement of dose using the NMR technique. The motivation behind the research in this field is to ultimately develop a practical dosimeter material which, together with NMR or MRI, could be used for three dimensional dose

determinations. However, the basic physical processes which describe the NMR behavior of irradiated Fricke solution have not been well established. Gore et al. (1984) have made the most elaborate attempt to formalize the basic physics of irradiated Fricke solutions, however, not all the basic NMR parameters of the solutions have been quantified. The research reported in this thesis is an attempt to better comprehend and to quantify some of the inherent parameters which govern the spin relaxation behaviour of irradiated Fricke solutions. The ultimate goal of this research is to establish the NMR technique as an absolute dosimetry technique based on an independent measurement of the chemical yield of ferric ions in irradiated Fricke solutions.

CHAPTER 3

EXPERIMENTAL

3.1 APPARATUS

3.1.1 The NMR system

The measurements were made using an NMR system comprised of a JELCO (Japanese Electronics Company, Tokyo, Japan) electromagnet obtained from the University of Waterloo, a home built pulse programmer, and a WNS (Waterloo Nuclear Spectrometer, Waterloo, Ontario) spectrometer operating at a Larmor frequency of 25 MHz.

The pulse programmer, constructed by the technical staff of the Medical Physics department at the Montreal General Hospital, provides a train of two pulses, as shown in Fig. 3. The heart of the device is centred around two TTL timer chips which enable different delays ranging from 10 μs to 990 s between the pulses (TI) and groups of pulses (TR). The duration of each pulse (t_a or t_b) is controlled by a monostable multivibrator and can be varied from 1 to 10 μs. The internal clock is provided by a 25 MHz crystal and the output of the programmer is amplified with transistors to ~ 4.1 V in order to trigger the spectrometer.

The spectrometer acts as a transmitter of the radiofrequency (r.f.) pulses and receiver of the induced NMR signal. The transmitter part consists of a quartz crystal which provides a stable

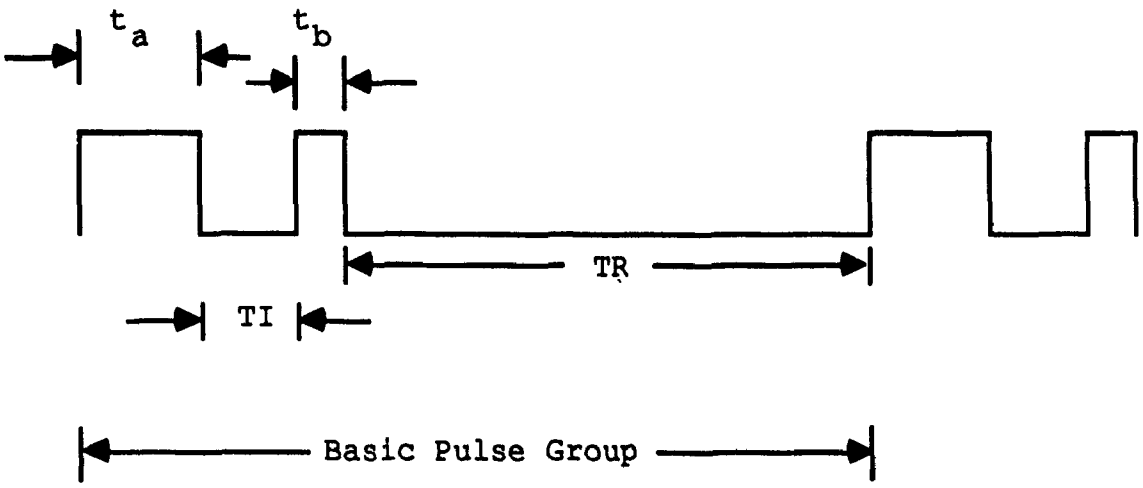

Figure 3 : Diagrammatic representation of the pulse sequence supplied by the pulse programmer. The basic sequence consists of two pulses of lengths t_a and t_b separated by time TI and repeated after time TR. Typically, $t_a \sim 7.5\ \mu s$, $t_b \sim 3.75\ \mu s$, TR ~ 8 s, and $10\ ms \leq TI \leq 8\ s$.

continuous radio frequency of 25 MHz which is gated and amplified such that r.f. pulses are sent to the transmitter. The gating is provided by the pulse programmer. The receiver amplifies the signal obtained from the sample and removes the r.f. carrier envelope. The sample is placed into a probe consisting of a solenoidal coil which couples the r.f. signal from the spectrometer with the sample. Since the NMR signal from the sample is in the microvolt range but the transmitter signal is of the order of a hundred volts it is necessary to decouple the receiver from the transmitter. This is done using the signal matching network included in the circuit between the spectrometer and the NMR probe.

The NMR signal was recorded on a Tektronix 2221 digital storage oscilloscope (Tektronix, Inc., Beaverton, Oregon). Details concerning the data acquisition techniques are described in §3.3.

3.1.2 Sample Irradiation

Irradiations were performed in the Department of Radiation Oncology at the Montreal General Hospital using a Theratron 780 (AECL, Ottawa, Ontario) cobalt-60 teletherapy unit. The unit is comprised of a treatment head, inside of which is the radioactive source, mounted to a rotating gantry with an isocentre of rotation at a distance of 80 cm from the source. The radiation field is delineated by continuously adjustable collimators which provide precise beam definition. For a cobalt beam, the depth where the maximum dose is deposited in phantom, known as d_{max}, is 0.5 cm. The dose rate at d_{max} in a tissue equivalent phantom for a 10x10 cm^2

field and a source-to-surface distance (SSD) of 80 cm was 107.1 cGy/min on April 1, 1989. The calibration of the cobalt unit was accomplished with an NPL secondary standard chamber and reader (Nuclear Enterprises Ltd., Beenham, England), the responses of which are traceable to the National Research Council in Ottawa, Canada.

The beta decay of Co-60 can follow two paths (Johns and Cunningham, 1983). Most of the disintegrations (99.8 %) are an allowed transition with the emission of a beta particle with a maximum energy of 0.313 MeV. This results in an excited state of Ni-60 which decays very quickly through the emission of two gamma rays in cascade, with energies of 1.173 and 1.332 MeV. In a few of the initial disintegrations (0.12 %) a second beta particle with a maximum energy of 1.486 MeV, is emitted, leading to the lowest excited state of Ni-60, however, the useful radiation in a Co-60 therapy unit is provided by the two gamma rays. The cobalt beam is considered to be monoenergetic with an effective energy of 1.25 MeV.

A schematic diagram of the irradiation geometry is shown in Fig. 4. All irradiations were performed in phantom in order to maintain electronic equilibrium between the dosimeter solution and its surroundings. The phantom used in the experiments was made of lucite and was mounted on a lucite tray such that it could be placed in the treatment head of the cobalt unit at a distance of 51.2 cm from the source. Three holes were drilled into the phantom enabling the simultaneous irradiation of three samples. The holes were at a depth of 1.5 cm in phantom and there was approximately 6 cm of lucite

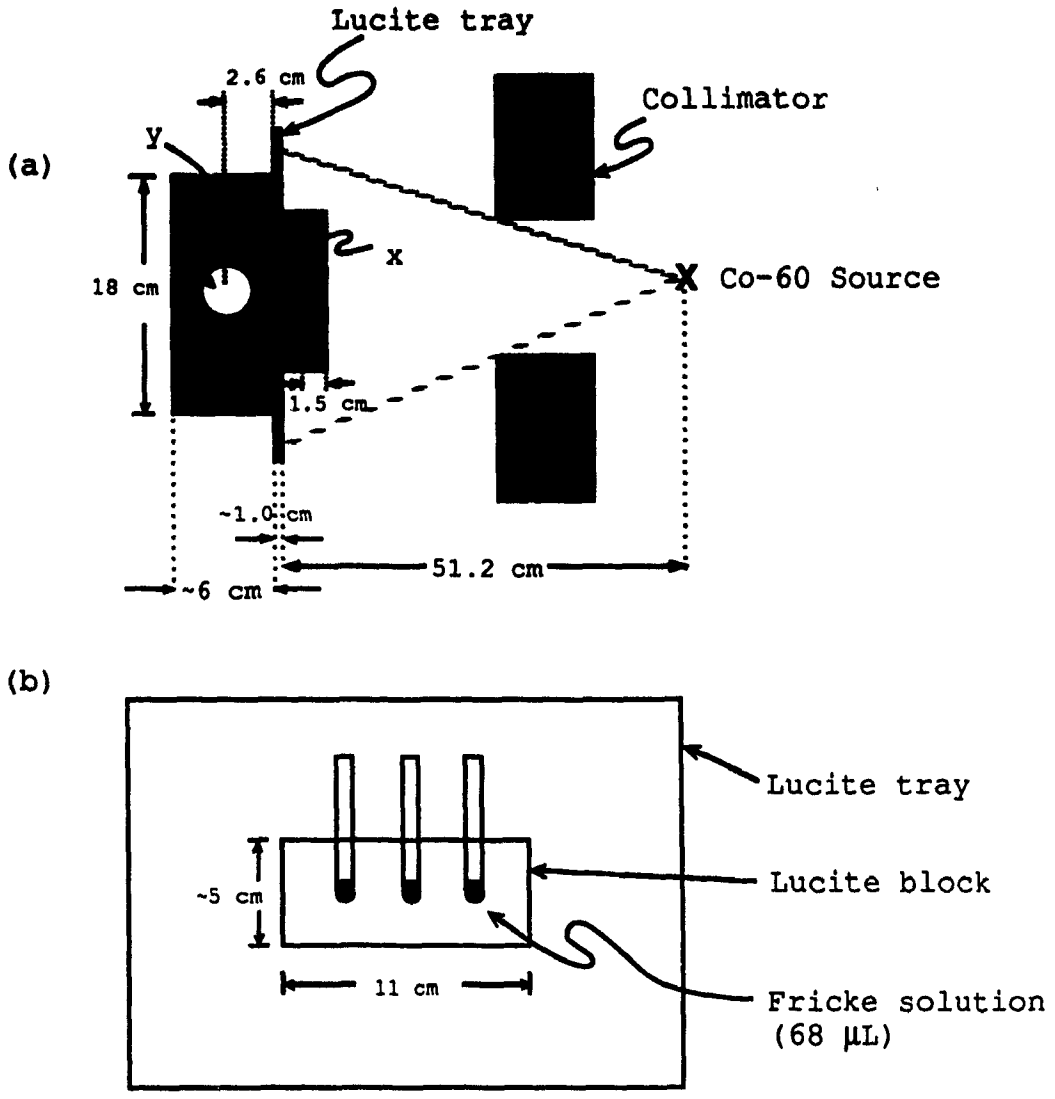

Figure 4: (a) Schematic diagram showing the geometry for the irradiation of either 68 µL (hole x: diameter = 0.6 cm) and 10000 µL (hole y: diameter = 2 cm) samples of Fricke solution. When irradiating the smaller volume solutions, hole y was filled with a lucite plug. (b) View from source position of the irradiation phantom. The 6 cm thick backscatter lucite block is not shown. The diagrams are not drawn to scale.

behind the holes to provide backscatter. The dose rate determination for each sample position in the phantom is described in the next section.

3.1.3 Dose rate determination

The dose rate at each sample position in phantom was found using the thermoluminescent dosimetry technique. Thermoluminescence (Cameron et al., 1968) can be briefly described as a particular form of phosphorescence whereby radiation incident on a material has some of its energy absorbed, i.e., a dose is deposited in the material. This absorption occurs in lattice defects which trap the secondary electrons which result from the interactions between radiation and the thermoluminescent material. The lattice defects can be emptied by increasing the temperature of the material. The stored energy is re-emitted in the form of visible or ultraviolet light and the amount of light emitted can be correlated to the radiation dose absorbed by the dosimeter. The thermoluminescent method is a standard dosimetry technique used extensively in many radiotherapy departments.

Lithium fluoride crystals, known as TLD-100 (Harshaw Chemical Co., Solon, Ohio), were used as the dosimeter material. The crystals were first irradiated in the cobalt beam at a reference position with a known dose rate, i.e., at d_{max} in a standard polystyrene calibration phantom with an SSD of 80 cm and a 10x10 cm^2 field. The calibration factor for the particular crystals used was determined by correlating the amount of light emitted by the heated crystal to the absorbed dose to water at the position of the crystal. Three TLD-100

crystals were irradiated in the phantom and the absorbed dose was determined using the calibration factor previously found. This procedure was repeated three times and the average dose rate at the sample holes was found to be 2.5 Gy/min on April 1, 1989. The dose rate on subsequent days was calculated using the measured dose rate quoted above and the half-life of Co-60 (5.3 years).

3.2 SAMPLE PREPARATION

The basic constituents of Fricke solution, as described in Chapter 2, are ferrous ions (Fe^{2+}), sulfuric acid, and sodium chloride. The ferrous ion was obtained from aqueous ammonium iron(II) sulfate hexahydrate (Aldrich Chemical Co., Milwaukee, Wisconsin) of 99+% purity. The sodium chloride (ACP Chemical Co., Montréal, Québec) and sulfuric acid (ACP Chemical Co., Montréal, Québec) were reagent grade. Ferric ion (Fe^{3+}) was obtained from aqueous ferric sulfate (Anachemia, Montréal, Québec) and was also reagent grade. The ferric sulfate was used to mimic irradiated Fricke solution (see Chapter 4). The water used was triply distilled.

3.2.1 Treatment of glassware

All glassware was cleaned according to the following procedure. First, the glassware was rinsed with triply distilled water to remove any macroscopic impurities. The glassware was then washed with sulfuric acid to remove microscopic organic impurities and rinsed again three times with distilled water. To remove paramagnetic impurities, some of the glassware was cleaned using the procedure

outlined by Peemoeller (1980). The glassware was immersed in a 1:1 mixture by volume of nitric and sulfuric acid for 12 hours, rinsed with distilled water, immersed in a 0.01 M solution of EDTA (Aldrich Chemical Co., Milwaukee, Wisconsin) for another 12 hours and then rinsed 10 times with distilled water. The paramagnetic impurities are bound by EDTA, therefore rinsing with EDTA should remove any such impurities from the glassware. Following rinsing with EDTA, a few sample tubes were also baked at 400°C for 24 hours to remove organic films from the glass.

Experiments were performed with glassware cleaned using the three techniques outlined above - simple cleaning with water and sulfuric acid, further rinsing with EDTA, and baking. It was found that the extra cleaning procedures using EDTA and baking produced no differences in the results. Therefore it was deemed sufficient to simply rinse once each with distilled water and sulfuric acid, and then three more times with distilled water.

3.2.2 Sample size

The volume of solution to be analyzed in a sample tube is limited by the size of the r.f. coil in the NMR system. Close to the edges of the coil, the r.f. field is perturbed relative to that in the center of the coil. The entire sample must be within a homogeneous region of the radiofrequency field, hence it is recommended (Fukushima and Roeder, 1981) that the sample be within the middle third of the coil. Following this recommendation, the maximum length of solution in the sample tube was 8 mm corresponding to a volume of 68 µL. Smaller samples result in a lower signal-to-noise ratio.

Most of the experiments were performed with the Fricke solution analyzed and irradiated in the same Pyrex sample tube (Fisher, Montréal, Québec), hence the volume of solution was limited to 68 μL. Modification of the phantom allowed a larger volume of solution to be irradiated, however, because of the coil limitations described above only 68 μL of the solution could be analyzed at a time.

3.3 SPIN-LATTICE RELAXATION TIME MEASUREMENT

As discussed in Chapter 1, a sample placed into a magnetic field will have a resultant magnetization, known as the longitudinal magnetization, $\mathbf{M}_o = M_o\hat{\mathbf{z}}$, parallel to the main magnetic field $\mathbf{H}_o$ supplied by the magnet. This magnetization is stable and will remain parallel to $\mathbf{H}_o$ until some external perturbation causes a re-distribution of the spin states within the sample. As previously mentioned, one way of changing the spin state distribution is by applying an r.f. pulse. The re-distribution of spin states caused by the time dependent magnetic field created by the r.f. pulse can be described as a tipping of the macroscopic magnetization away from the equilibrium direction $\hat{\mathbf{z}}$. The magnetization now also has a component, known as the transverse component, in the xy plane. The angle between the equilibrium magnetization and the magnetization after the r.f. pulse is applied depends upon the pulse length and height. A π pulse, for example, tips the magnetization through π radians, or 180° and, similarly, a $\pi/2$ pulse with the same height tips the magnetization through 90°.

Since the spin-lattice relaxation time (T_1) describes the dynamics of the re-establishment of the equilibrium spin distribution, T_1 is related to the evolution of the longitudinal magnetization subsequent to the application of the perturbation. Therefore the magnetization in the $\hat{z}$ direction must be monitored when determining the T_1 of a sample. However, the axis of the receiving/transmitting coil is perpendicular to the $\hat{z}$ axis, i.e., it is in the xy plane. Therefore, only the transverse magnetization component can in fact induce a current in the coil and be measured. Hence, it is necessary to measure the longitudinal magnetization component indirectly by measuring the transverse magnetization component and then relating it to the longitudinal component. The technique is outlined below.

The r.f. pulse sequence used to measure the spin-lattice relaxation time in the experiments performed for this thesis was the inversion recovery sequence. The main features of this pulse sequence are outlined in Fig. 5 and they can be schematically represented as:

$$\pi \text{ pulse} - \text{TI delay} - \pi/2 \text{ pulse} - \text{Data acquisition} \qquad (3.1)$$

where signal acquisitions are made for several TI's.

The π pulse prepares the macroscopic magnetization while the $\pi/2$ pulse measures the magnetization after a certain waiting period. The preparatory π pulse inverts the magnetization such that it is antiparallel to $\mathbf{H}_o$; the magnetization becomes exactly $-\mathbf{M}_o$ and there

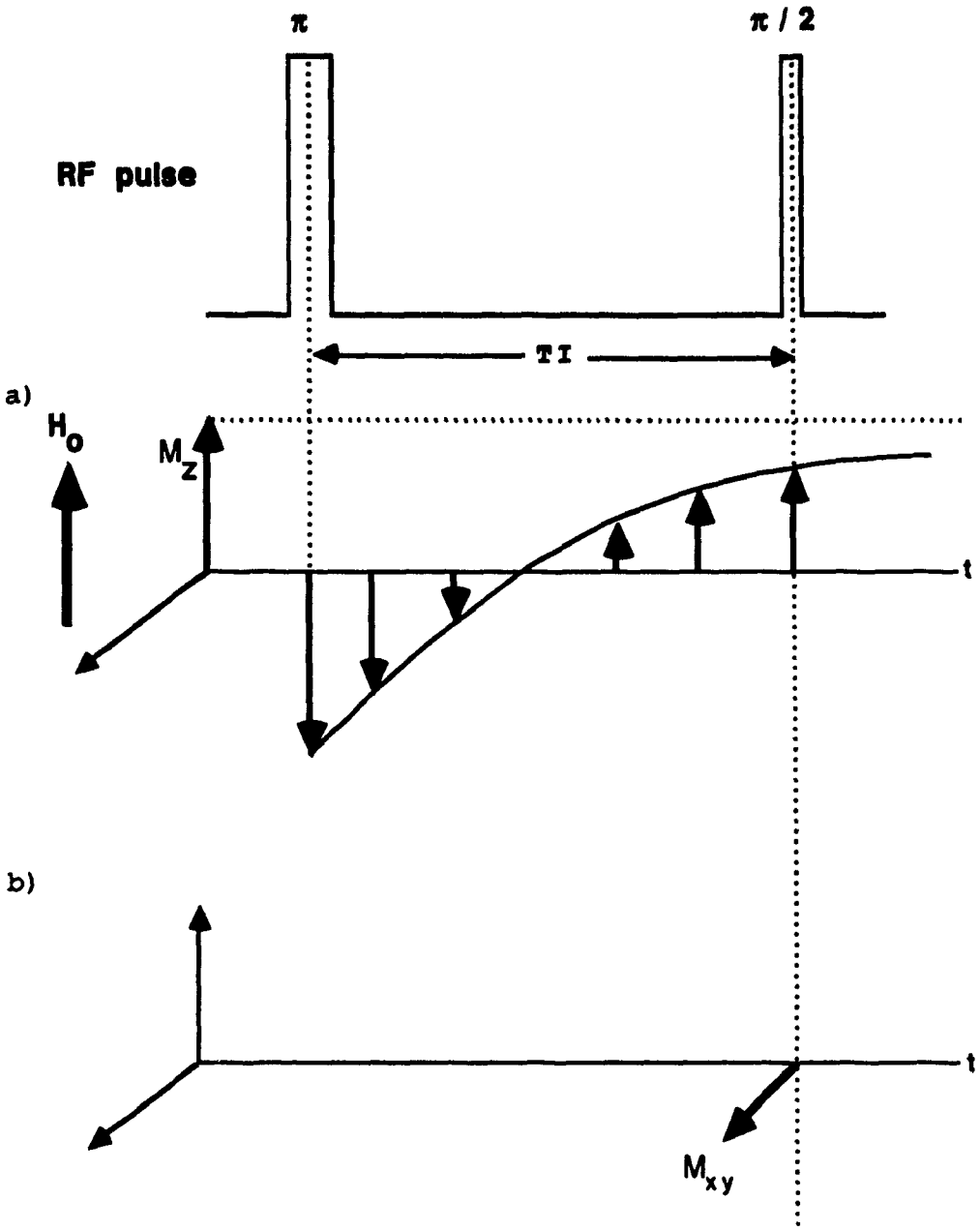

Figure 5 : Diagrammatic representation of the evolution of (a) the longitudinal (M_z) and (b) the measured transverse (M_{xy}) magnetizations irradiated with the r.f. pulses of an inversion recovery sequence. The external magnetic field is H_o.

is no transverse magnetization, hence it is not possible to directly observe the effect of the pulse. In fact, this feature of the π pulse is used to set the pulse length. As stated above, to monitor the magnetization it is necessary to create a transverse component which can induce a current in the coil. This is accomplished by applying a $\pi/2$ pulse some time TI after the π pulse. Just before application of the $\pi/2$ pulse, the longitudinal magnetization has relaxed towards its equilibrium direction. The $\pi/2$ pulse then rotates the magnetization by 90° creating a transverse component equal in magnitude to the longitudinal component which was present just before the $\pi/2$ pulse was applied. Thus, the current which is induced in the coil after the $\pi/2$ pulse is applied produces a signal A(TI) which is proportional to the longitudinal magnetization. The experiment is repeated several times with different TI delays. The recovery of the amplitude, proportional to the relaxation of the longitudinal magnetization, is of the form

$$A(TI) = A_{\infty} [1 - 2 \exp(-TI/T_1)] , \qquad (3.2)$$

where A_{∞} is the signal obtained for infinite TI.

The spin-lattice relaxation time T_1 was determined from a semilogarithmic plot of the reduced magnetization $[A_{\infty}-A(TI)]/2A_{\infty}$ versus TI, as shown in Fig. 6. For all samples studied, this plot was linear, hence the relaxation was monoexponential and it could be concluded that the samples behaved as a homogeneous system (see §4.3.1). A linear fit of this plot has a slope of $-1/T_1$. Analysis of Fig. 6 shows that the two samples had markedly different relaxation behaviors, with sample (a) having the longer T_1. The data

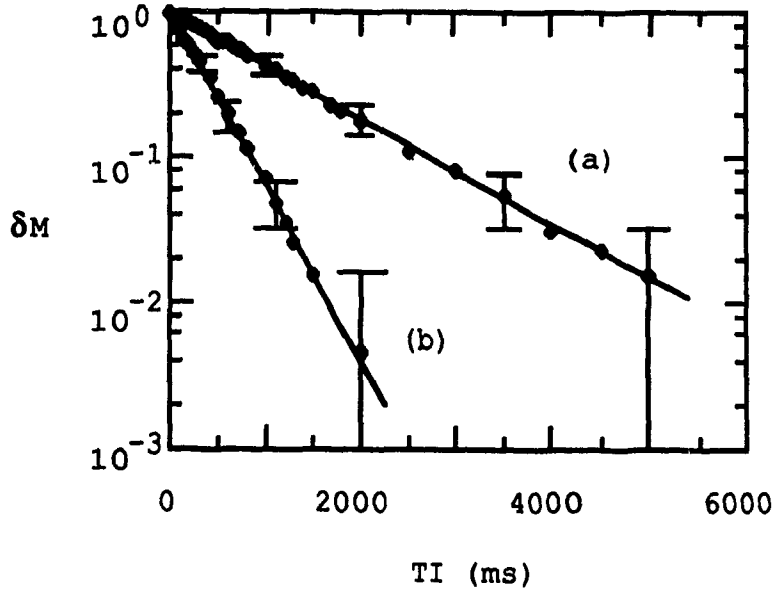

Figure 6 : The reduced magnetization $\delta M(TI) = [A_\infty - A(TI)]/2A_\infty$ plotted as a function of the delay time TI for (a) unirradiated Fricke solution and (b) Fricke solution irradiated to 100 Gy.

were analyzed on a Macintosh Plus (Apple Computer Inc., Cupertino, California) personal computer using software developed in the NMR laboratory at the Montreal General Hospital. The linear regression fit included readings up to ~96 % of the maximum amplitude, i.e., the fit was made up to a delay time TI resulting in a magnetization which had almost fully relaxed back to equilibrium. The fitting routines were based on a weighted fit of logarithmic data (Bevington, 1969) and the measured error in each amplitude reading was found to be constant at 2 percent.

To maximize the signal-to-noise ratio (S/N), the measured signal amplitude for each TI was acquired ten times and then averaged. Typically, this averaging process improved the S/N from about 15:1 to approximately 50:1. The time base of the data acquisition scope was set such that the signal could be viewed for 100 μs after application of the π/2 pulse. The dead-time of the system was 16 μs and the signal amplitude was read 30 μs after the π/2 pulse. This did not introduce any errors since the samples studied were liquids with spin-spin relaxation times (T_2) of approximately 8 ms hence there was no visible signal decay in the first 100 μs after the application of the π/2 pulse. The base-line was taken as the signal amplitude just before the π/2 pulse was applied; this amplitude corresponded to the signal with no sample in the coil. A second oscilloscope set at a 1ms time-base was used to observe the signal after the π pulse to ensure that the magnetic field maintained proton resonance during the data acquisition. If the magnetic field did in fact drift such that the protons precessed at a frequency different from the spectrometer frequency, the magnet current could be re-adjusted and the data re-acquired.

CHAPTER 4

DISCUSSION

4.1 SPONTANEOUS OXIDATION OF FERROUS ION

Aerated ferrous ions in solution slowly oxidize to ferric ion. This oxidation proceeds at a rate which is proportional to both the square of the ferrous ion concentration and the first power of the oxygen concentration (Huffman and Davidson, 1956). An experiment was performed in order to determine the rate of spontaneous oxidation of the Fricke solution dosimeter. The spin-lattice relaxation time of unirradiated modified Fricke solution was monitored for three months. It was found that the T_1 of the unirradiated solution decayed at a rate of 3 ms/day. Since the spontaneous decay rate is proportional to the square of the ferrous concentration and the first power of the oxygen concentration, it is expected that irradiated Fricke solution, containing lower ferrous and oxygen concentrations, will have a smaller decay rate. This was in fact experimentally observed; the T_1 of modified Fricke solution irradiated to 50 Gy was found to decay at a rate of approximately 1 ms/day. Unless the oxidation is allowed to continue over many days, the spontaneous oxidation of ferrous to ferric ion in the Fricke dosimeter is not significant; particularly, if the Fricke solution is irradiated and probed within a few days of preparation, the change in T_1 due to the spontaneous oxidation can be neglected. In experiments performed for this thesis, Fricke solutions were used within 2 days of mixing and their relaxation rates were determined within two hours of irradiation.

4.2 NMR ANALYSIS OF IRRADIATED FRICKE SOLUTION

4.2.1 Modified Fricke solution

As described in Chapter 2, radiation impinging on a solution of aqueous ferrous ions results in the oxidation of ferrous ions to ferric ions. There are a number of physical differences between ferrous and ferric ions which are important with respect to nuclear spin relaxation. Equation (1.18) shows that the relaxation rate of a paramagnetic solution is dependent on the gyromagnetic ratios of the proton and electron spins, the spin state of the paramagnetic ion, and the correlation times for electron relaxation and the rotational motion of the ion. Ferrous and ferric ions differ in all of the above variables (Eisinger et al., 1961), therefore the two ions should also differ in their ability to enhance proton relaxation in ionic solutions. The ferric ion is a more efficient relaxation sink than the ferrous ion.

Because of the different efficiencies for promoting proton relaxation between ferrous and ferric ion, solutions containing both ions but at different concentrations will have marked differences in their relaxation times. Since the ferrous ions are oxidized to ferric ions in the irradiated solution, the relative concentration of each ion in solution depends upon the absorbed dose. Therefore the relaxation time of Fricke solution also depends upon the dose absorbed by the solution. The dependence of the spin-lattice relaxation rate of modified Fricke solution on radiation dose is shown in Fig. 7. The irradiation was performed according to the

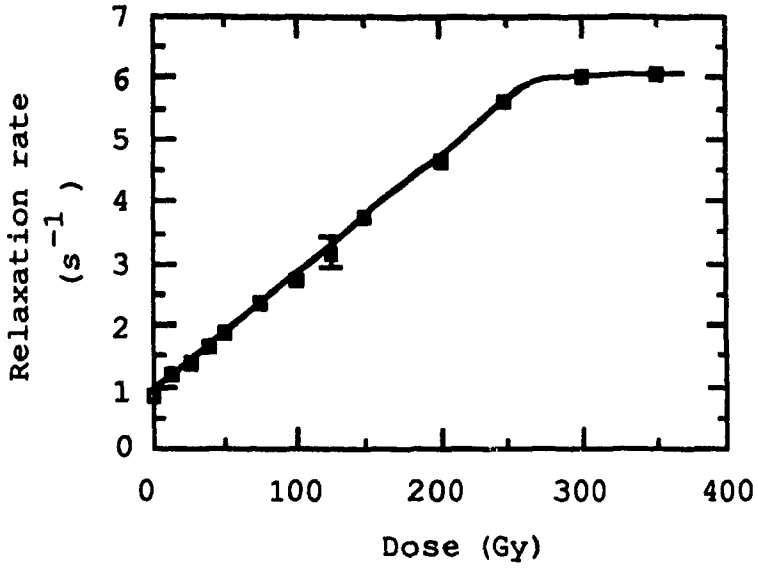

Figure 7 : Measured spin-lattice relaxation rate of modified Fricke solution as a function of absorbed radiation dose. The linear part of the solid line is a least squares fit of the data and numerically represents the NMR sensitivity of the dosimeter. A representative error bar is shown.

procedure outlined in Chapter 3. Modified Fricke solution was made using the usual recipe (1 mM Fe^{2+}, 1 mM NaCl, and 0.8 N H_2SO_4). A linear relation was found between the spin-lattice relaxation rate and the absorbed dose up to ~250 Gy. The slope of the linear portion of Fig. 7, termed the NMR sensitivity of the Fricke solution to radiation, is 0.0182 ± 0.0004 $s^{-1}Gy^{-1}$. This value is in excellent agreement with the NMR sensitivity to radiation of aqueous Fricke solution reported by Szeredi et al. (1986) and Olsson et al. (1988).

At doses higher than 250 Gy, the dose response of the Fricke solution is no longer linear and the change in the relaxation rate with increasing dose saturates. This is a result of the progressively lower concentration of dissolved oxygen in the solution as the irradiation proceeds. The reactions which result in the oxidation of ferrous ions require a supply of oxygen dissolved in the solution. As the Fricke solution is irradiated, the chemical reactions which oxidize the ferrous ions consume the dissolved oxygen at a constant rate. Eventually the concentration of oxygen is no longer sufficient for the reactions to proceed at the same rate and the chemical yield for ferric ion begins to decrease. The removal of oxygen at high doses also affects the spin-lattice relaxation of the solutions (see below). Ultimately, all the ferrous ions are depleted by the radio-chemical reactions and additional ferric ions are not produced as the irradiation continues. At this stage the relaxation rates remain constant as the absorbed dose is increased.

The reproducibility of the dose response of the modified Fricke solution was investigated. Samples from eight different solutions were irradiated to 25 and 50 Gy. The relaxation rates of the

irradiated samples, as well as of an unirradiated sample from each batch, are plotted in Fig. 8. The standard deviation of the relaxation rate measurements for samples of different solutions irradiated to 0, 25 Gy, and 50 Gy are 0.02 s^{-1}, 0.04 s^{-1}, and 0.03 s^{-1}, respectively. These errors are less than the precision of each specific relaxation rate measurement, therefore it can be concluded that the Fricke solution can be prepared reproducibly.

The reproducibility in the relaxation rate measurement for different Fricke solutions quoted above, however, can only be achieved if very careful preparation procedures are followed. Initially, the standard deviations of the relaxation rates between different samples were larger than the precision of the NMR system, and it was not until the very specific cleaning and mixing protocols described in Chapter 3 were implemented that the inter-sample reproducibility was deemed acceptable.

4.2.2 Effect of NaCl

Careful cleaning of all glassware used to prepare a chemical dosimeter is essential, however, it may not be sufficient. Organic impurities may be introduced into the chemical solutions at various points, even after thorough macroscopic cleaning procedures have been followed. The impurities may be present in the distilled water or in the constituent chemicals which comprise Fricke solution, or they may be released from the glassware as it is irradiated. In order to determine the extent of contamination of the solutions, the relaxation rate versus absorbed dose curve for modified Fricke solution (containing NaCl) was compared to that obtained for standard

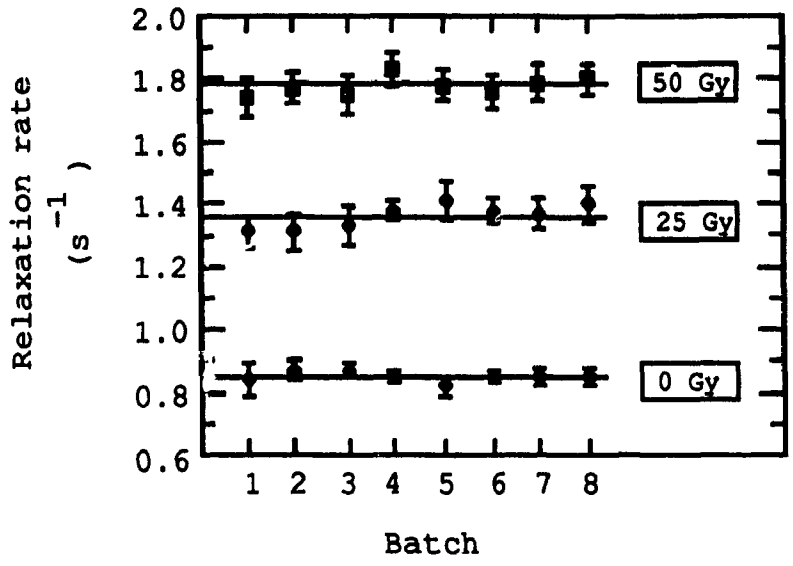

Figure 8 : Measured spin-lattice relaxation rates for eight batches of Fricke solution prepared over a period of 7 months. Unirradiated samples and samples irradiated to 25 Gy and 50 Gy were analyzed. The solid line through the points indicates the mean spin-lattice relaxation rate.

Fricke solution (without NaCl). The results are shown in Fig. 9. The relaxation rates of unirradiated samples of the modified and standard Fricke solutions were identical, however, the sensitivity of the standard Fricke solution was about 11 percent higher than that of the modified solution. This difference in sensitivity, implying a difference in the chemical yields, suggests that although very careful cleaning procedures were followed, impurities still contaminated the solutions. Hence, to minimize the variability in the NMR sensitivity of Fricke solution due to organic impurity contamination, modified Fricke solution was used in all further experiments. The chloride ion (Cl^-) protects the modified solution from the increase in chemical yield which results from organic impurity contamination. In the absence of impurities the chloride ion lowers the chemical yield by less than 1 percent (Cottens et al., 1982; Simoen, 1978; Davies and Law, 1963; Shalek and Smith, 1969).

4.3 NMR RELAXATION MEASUREMENTS AS AN ABSOLUTE DOSIMETER

For doses below 250 Gy, the spin-lattice relaxation rate of Fricke solution is directly proportional to the dose. Also, the chemical reactions describing the oxidation of ferrous ions to ferric ions in irradiated Fricke solution suggest that there is a direct proportionality between the absorbed dose and the amount of ferric ions produced. In fact, the chemical yield of ferric ion is well established (Attix et al., 1966). Therefore, if the spin-lattice relaxation rate of Fricke solution can be related to the ferric ion

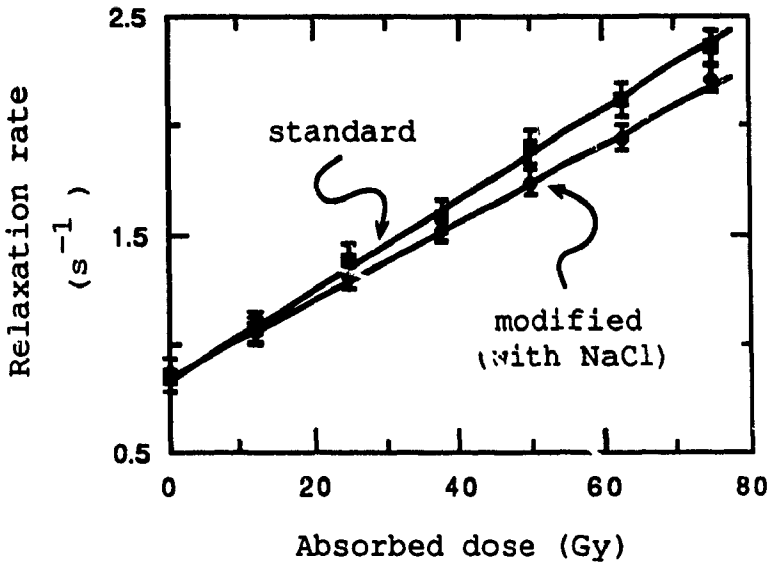

Figure 9 : Dose dependence of the spin-lattice relaxation rate of standard and modified (with 1 mM NaCl added) Fricke solutions. The solid lines are least square fits of the data from which the NMR sensitivities of the solutions are determined: 0.0182 and 0.0210 $s^{-1}Gy^{-1}$ for the modified and standard Fricke solutions respectively.

concentration, the NMR-Fricke measurement of dose would satisfy the criteria for an absolute dosimetry technique; i.e., the absorbed dose could be calculated directly from the NMR spin-lattice relaxation time and some basic physical quantities. It is with this motivation that a model describing the NMR spin-lattice relaxation of Fricke solutions is described below. The model, initially proposed by Gore et al. (1984), is based on the NMR relaxation of protons on water molecules which are exchanging between three different environments. In this thesis, the model is further developed and the results of experiments to determine the inherent NMR parameters of the model are reported.

4.3.1 Exchange modelling of the NMR spin-lattice relaxation

Even though Fricke solution contains both ferrous and ferric ions, it is instructive to begin the description of the exchange model of the NMR spin-lattice relaxation with separate solutions of either ion. In an aqueous solution of ferrous (or ferric) ions, water molecules exist in two different environments. Some water molecules are in the coordination shells of ions (termed, for this thesis, bound water molecules) and the others are in the bulk. The protons on the bound water and the bulk water protons relax by different mechanisms (see Chapter 1). The bound water protons experience the enhanced relaxation resulting from the local paramagnetic centres while the bulk water protons have relaxation rates characteristic of pure water. The two proton environments are mixed because of diffusion of water molecules between the coordination shell of the ion and the bulk. Therefore, as discussed previously, the measured spin-lattice relaxation rates for a solution

of paramagnetic ions is a function of the inherent relaxation rates of bulk and bound water molecules, the fraction of protons in each water group and the exchange rates between the two environments. The exchange of water molecules between the two environments is assumed to be very fast so that the exchange modified spin-relaxation is in the fast exchange limit (Hertz, 1973; Gore et al., 1984). The apparent spin relaxation rate of a heterogeneous spin system with exchange in the fast exchange limit is the weighted average of the inherent relaxation rates of the different spin groups of the system. Thus the observed relaxation rate of a solution of either ferrous or ferric ions can be written as:

$$R_T = p_b R_{in} + (1 - p_b) R_w , \qquad (4.8)$$

where p_b is the fraction of protons in the solution which are on water molecules in the coordination shell of the ion, R_{in} is the inherent relaxation rate of the protons on these bound water molecules, and R_w is the relaxation rate of the bulk water protons.

The fraction of protons on water molecules which are in the coordination shell of an ion is assumed to be proportional to the concentration of ion [C] in the solution:

$$p_b = k [C]. \qquad (4.9)$$

The k is a proportionality constant related to the number of water molecules associated with each ion. Equation (4.9) is valid since the number of water molecules in contact with each ion throughout the solution is constant. The bound water fraction p_b discussed above is

identified with the first hydration sphere of the ion only. It is assumed that the ionic concentrations of the solutions are low enough that there is no overlap between the hydration spheres of neighbouring ions; therefore, the constant ℓ in Eq. (4.9) is related directly to the coordination number n_h which gives the number of water molecules in actual contact with the ion: $\ell = n_h/55.5\ M^{-1}$, where 55.5 mol/L is the molarity of water (Deverell, 1969). The spin-lattice relaxation of the protons on the water molecules in the higher order hydration spheres surrounding the ion is not expected to contribute significantly to the relaxation of the total spin mass of the solutions (see below) and so these protons are not accounted for in Eqs. (4.8 and 4.9). As is typical for most divalent and polyvalent ions (Deverell, 1969; Horvath, 1985) the coordination number for ferrous and ferric ions is six at the low pH of the solutions used in this study (Cotton and Wilkinson, 1966). Therefore, in the aqueous solutions studied here, $\ell = 1.08 \times 10^{-4}\ mM^{-1}$ for both ions.

In Eq. (4.8) it is implied that the spin-lattice relaxation of only the water protons in the first hydration shell is perturbed by the paramagnetic ion. The activation energy for the binding of the water molecules in the first hydration sphere of either ion is approximately 9 kcal/mol (Genser, 1962; Swift and Connick, 1962). Therefore, these water molecules are bound to the ion and have a fixed residence time in the first hydration sphere (see below) during which they are affected by the unpaired electron spins of the paramagnetic ion. One might also expect some interaction between the ion and the water protons in higher order hydration spheres. However, the paramagnetic ion-proton interactions will be less

significant than that of the first shell since the distances between the ion and the protons is increased and the interaction goes as r^{-6}. Also, the dynamics of the coupling changes: the water molecules in the higher order hydration spheres do not bind to the ion for any substantial amount of time (Hertz, 1973) and the time dependence of the dipolar coupling is the result of translational diffusion of the water molecules about the ions. Detailed discussions of outer sphere effects can be found in the literature (Dwek, 1975; Koenig and Epstein, 1975; Pfeifer, 1962; Hauser and Noack, 1965) and are beyond the scope of this thesis. The point of interest for this thesis is that the contribution from the outer shells is minimal. It is estimated that the contribution to the total spin-lattice relaxation from water molecules in the outer shell of an ion is less than 6 % (Dwek, 1975) or 10 % (Koenig and Brown, 1984). On the other hand, water molecules in the first hydration shell dominate the apparent relaxation processes. Therefore, in this work the explicit contribution to the apparent spin relaxation of the ionic solutions from the higher order hydration spheres is ignored.

Equation (4.8) can be written as

$$(R_T - R_w) = \beta\,[C]\,(R_{in} - R_w)\ , \qquad (4.10)$$

which directly relates the concentration of the ferrous or ferric ion to the measured spin-lattice relaxation rate R_T. The spin-lattice relaxation rate of the bulk water R_w is known: for pure water R_w is 0.28 s^{-1} (Hertz, 1973). The R_w of the triply distilled water used in the experiments performed for this thesis, however, was measured as 0.42 s^{-1}. The discrepancy between the measured rate and the rate for

pure water is the result of impurities, mostly dissolved oxygen, which are present in the water (Fukushima and Roeder, 1981). Oxygen is paramagnetic and, just like any other paramagnetic impurity, it enhances the relaxation rate of the water. Glasel (1972) has shown that oxygen dissolved in water causes an increase of up to 40 % in the spin-lattice relaxation rates compared to degassed water. The oxygen dissolved in the water used in these experiments was not extracted since the Fricke reaction mechanism requires oxygen and the dosimeter solutions had to be aerated. The perturbation of the total apparent spin-lattice relaxation of the ionic solutions introduced by using aerated water will be shown below to be negligible in the linear region of Fig. 7.

To quantify Eq. (4.10), the spin-lattice relaxation rates of aqueous solutions with concentrations of ferrous and ferric ions varying from 0.01 mM to 100 mM were measured at a constant pH of 1. (The requirement of low pH is discussed below.) The data are presented in Fig. 10 as plots of $(R_T - R_w)$ versus the ionic concentration [C] for separate aqueous solutions of ferrous (Fe^{2+}) or ferric (Fe^{3+}) ions. The data for aqueous Fe^{3+} agree with those from experiments performed by Solomon (1955). The solid lines in Fig. 10 show least square linear fits of the measured data. The slopes of these lines, representing the increase in the relaxation rate per unit concentration of either ion, are defined to be the constants f (for the Fe^{2+}) and g (for the Fe^{3+}), i.e., $f = \ell\, [R_{in}{}^{2+} - R_w]$ and $g = \ell\, [R_{in}{}^{3+} - R_w]$. From Fig. 10, $f = 0.45 \pm 0.01\ s^{-1}mM^{-1}$ and $g = 7.98 \pm 0.08\ s^{-1}mM^{-1}$ for the ferrous and ferric ions, respectively. The constants can be put into more basic units using Avogadro's number

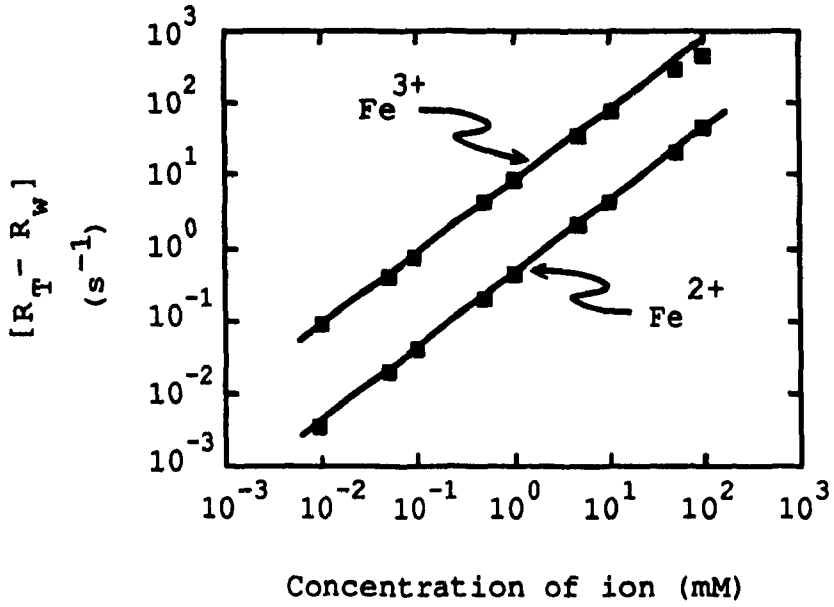

Figure 10: Concentration dependence of the relaxation rate enhancement ($R_T - R_W$) of ferrous (Fe^{2+}) and ferric (Fe^{3+}) ionic solutions relative to bulk water. The solid lines are least squares fits of the data used to determine the constants f and g.

and the molarity of water giving $f = (5.03 \pm 0.05) \times 10^4\ s^{-1}$ proton/ion and $g = (8.87 \pm 0.09) \times 10^5\ s^{-1}$ proton/ion.

If the acidity of the solutions is not kept constant at the low pH of 1, the increase in the relaxation rate is not directly proportional to the concentration of ions, and the analogous plot to Fig. 10 is no longer linear (Gore et al., 1984). As the pH is raised above 2, the iron ions form condensed complexes whose chemical compositions are dependent on the pH of the solution (Cotton and Wilkinson, 1966). The ferric and ferrous ions in these complexes have different water coordinations depending on the pH of the solution. The coordination number for water molecules surrounding these complexes, n_h, is not necessarily six at the higher pH's. Therefore, the parameters describing the exchange processes are pH dependent and the experimentally determined constants for the model proposed above will not adequately describe the spin relaxation of an ionic solution whose acidity is not kept below pH = 2. To maintain ferric and ferrous ions in the hexaquo ionic form ($n_h = 6$), it is recommended that the pH be close to 0 (Cotton and Wilkinson, 1966). Since Fricke solution exists at a pH of 1, it was decided to perform the experiments described above at a pH of 1. An added benefit of maintaining a low pH in Fricke solutions is that the spontaneous oxidation of ferrous ion proceeds at a lower rate than at higher pH (Cotton and Wilkinson, 1966).

The inherent spin-lattice relaxation rates R_{in}^{2+} and R_{in}^{3+} can be calculated from the fitted constants f and g since both k and R_w are known. The inherent rates for the water protons bound to the ferrous

and the ferric ions at 25 MHz are $R_{in}^{2+} = 4.17 \times 10^3\ s^{-1}$ and $R_{in}^{3+} = 7.39 \times 10^4\ s^{-1}$, respectively. The assumptions made in developing the model describing the spin-lattice relaxation of the ferrous and ferric ionic solutions can be validated using the theoretical equations for proton relaxation by paramagnetic centres discussed in Chapter 1. The inherent rates R_{in}^{2+} and R_{in}^{3+} are given by Eq. (1.18) for the ferrous and ferric ions, respectively. Equation (1.18) can be simplified since the electron spin resonance frequency ω_S is 658 times larger than the resonance frequency for a proton spin ω_I (Abragam, 1961), i.e. $\omega_S >> \omega_I$. Thus Eq. (1.18) can be written as:

$$R_{in} = \frac{2}{15} \frac{S(S+1)\, \hbar^2\, \gamma_I^2\, \gamma_S^2}{r^6} \left[\frac{3\tau_c}{1+\omega_I^2\tau_c^2} + \frac{7\tau_c}{1+\omega_S^2\tau_c^2} \right]. \qquad (4.11)$$

The correlation times τ_c for the ferrous and ferric ion are 1.5×10^{-12}s and 5.1×10^{-11}s, respectively (Eisinger et al., 1961), therefore at a proton NMR frequency of 25 MHz, $(\omega_S\tau_c)^2 << 1$ for the ferrous ion and $(\omega_S\tau_c)^2 >> 1$ for the ferric ion and the second term on the right hand side of Eq. (4.11) will differ depending on which ion is in solution. The dependence of the spin-lattice relaxation rate of either ionic solution on the NMR frequency can be shown by noting that for both ions at 25 MHz, $(\omega_I\tau_c)^2 << 1$. Incorporating this limit along with the appropriate electron spin limit ($(\omega_S\tau_c)^2$) into Eq. (4.11) gives

$$R_{in}^{2+} \approx \frac{1.98 \times 10^{18}}{r^6} \tau_c \qquad (4.12a)$$

$$R_{in}^{3+} \approx \frac{2.88 \times 10^{17}}{r^6} \left[3\tau_c + \frac{7\tau_c}{\omega_s^2\tau_c^2} \right], \qquad (4.12b)$$

where the constants 1.98×10^{18} and 2.88×10^{17} incorporate the factors $2S(S+1)\hbar^2\gamma_I^2\gamma_S^2/15$ for the ferrous (S=2) and ferric (S=5/2) ions, respectively and have units of $Å^6s^{-2}$. Equations (4.12) show that the spin-lattice relaxation of a solution of ferrous ions has no frequency dependence while the relaxation of a solution of ferric ions is dispersive around 25 MHz. These findings have been confirmed by Bloembergen and Morgan (1961) and Koenig and Brown (1984) for the spin-lattice relaxation of solutions of ferrous or ferric ions, respectively. It is understood, then, that the value of the inherent spin-lattice relaxation rate for the ferric ion, R_{in}^{3+}, is valid only for a proton NMR frequency of 25 MHz. The R_{in}^{2+}, although non-dispersive around 25 MHz, will have a frequency dependence above ~100 MHz.

The ratio of the inherent spin lattice relaxation rates for protons in the coordination shell of the two ions can be calculated from Eqs. (4.12) giving $R_{in}^{3+}/R_{in}^{2+} = 16.1\ (r^{2+}/r^{3+})^6$. It is this relation which quantifies the potential of the NMR method of measuring the relative concentration of ferric and ferrous ions in irradiated Fricke solution. Since the ratio of the ion-proton distances (r^{2+}/r^{3+}) is expected to be close to unity (see below), the ferric ion has an inherent relaxation rate which is approximately 16 times that of the ferrous ion. A small change in the ferric concentration, such as that produced by irradiating a sample of Fricke solution, will therefore produce a large change in the spin-lattice relaxation rate of the sample. The constant 16.1 which relates the ratio of the inherent spin-lattice relaxation rates to the ion-proton distances for the two ions differs slightly from that obtained by Gore et al. (1984) since they operated at 20 MHz.

The ion-proton distances r^{2+} and r^{3+} are the distances between the proton (hydrogen atom) on a water molecule which is in the first hydration sphere of an ion and the center of the ion itself. For the ferrous and ferric ions, the ionic radii are 2.12 Å and 2.04 Å respectively (Marcus, 1983, 1985). The radius of a water molecule is 1.4 Å, therefore the ion-proton distances r^{2+} and r^{3+} are 3.52 Å and 3.44 Å, respectively, and the ratio r^{2+}/r^{3+} is 1.023. The calculated ratio of the inherent relaxation rates is therefore approximately 18.5. Experimentally, the ratio of the inherent relaxation rates is determined to be 17.7 which differs only slightly from the theoretical value. This difference is a result of the fact that some approximations have been made in both the utilization of Eqs. (4.12) and in the empirical determination of the inherent spin-lattice relaxation rates. Firstly, the ionic radii used above are average values calculated from the crystal ionic radius. The actual radii of the ions in an aqueous electrolytic solution deviate from ideal crystal values because of the change in the electrical or coulombic attractions between the ions; therefore, the ionic radii and the ion-proton distances quoted above are only approximations (Horvath, 1985). Secondly, whereas the outer hydration shell contributions to the spin-relaxation are included in Eqs. (4.11 and 4.12), they are neglected in Eq. (4.10) thus causing some uncertainty in the values of the empirical inherent relaxation rates. However, in spite of these approximations, the experimental ratio between the inherent relaxation rates agrees very well with the theoretically derived value. Therefore, the inherent rates $R_{in}^{2+} = 4.17 \times 10^3\ s^{-1}$ and $R_{in}^{3+} = 7.39 \times 10^4\ s^{-1}$ are considered reasonable. A more complete analysis of the two site exchange model for the spin relaxation of the ferrous and ferric solutions could be undertaken with studies of the

temperature and frequency dependences of the spin-lattice relaxation rates of the solutions. This, however, is beyond the scope of the present work.

Since it has been shown that the inherent relaxation rates R_{in}^{2+} and R_{in}^{3+} have values predicted by theory, the assumption of fast exchange can be assessed. It may seem obvious that the bound and bulk water spin groups are in the fast exchange limit since experimentally, the spin-lattice relaxation of a solution of either ion is found to be monoexponential. (A typical magnetization recovery for a 1 mM ferrous ion solution is shown by the zero dose curve in Fig. 6.) However, the fraction of protons on the water molecules which are in the coordination shell of an ion is typically less than one percent of the total spin mass and are not resolvable with the current spectrometer which has a S/N of 50:1. Therefore one cannot invoke the fast exchange limit based solely on the shape of the magnetization recovery curve. The model can be justified with some other criteria. The lifetimes of water molecules in the first hydration spheres of ferrous and ferric ions are $\tau^{2+} = 3.1 \times 10^{-7}$ s (Swift and Connick, 1962) and $\tau^{3+} = 3.3 \times 10^{-4}$ s (Genser, 1962), respectively. If the inherent spin-lattice relaxation time for both proton groups is much longer than the lifetime of a water molecule in the first hydration sphere of an ion, then the spin system is definitely in fast exchange (Zimmerman and Brittin, 1957). This criterion is fulfilled for the ferrous ion solution. However, the ferric ion solution has an inherent relaxation time which is shorter than the lifetime of a water molecule in the hydration sphere of the ion and it is not entirely obvious from the Zimmerman-Brittin criterion that the ferric spin system is in fast exchange. Schreiner

and Podgorsak (1989) have shown, however, that the fast exchange limit occurs when $k/[p_b(R_{in}-R_w)] > 10$ where k is the exchange rate between water molecules in the hydration sphere of an ion and water molecules in the bulk, i.e., k is the inverse of the lifetime of a water molecule in the hydration sphere of an ion ($k = \tau^{-1}$). For the ferric spin system, this criterion is satisfied at all ionic concentrations lower than 50 mM so we can conclude that the ferric spin system is in fast exchange only at ferric ion concentrations less than 50 mM. The measured data shown in Fig. 10 indicate the range of ionic concentrations over which the fast exchange model is valid. According to Eq. (4.10), there should be a linear relationship between the rate difference $R_T - R_w$ of an ionic solution and the ionic concentration if the two spin groups involved are in fast exchange. This criterion of linearity is satisfied over the entire ferrous ion concentration range studied, however, for ferric ion concentrations higher than 50 mM, the linear relationship breaks down. Hence in calculating the slope of the solid line in Fig. 10 for the ferric ion (recall that this slope is equal to the constant g), data for concentrations higher than 50 mM were neglected. This apparent deviation of ferric ion solutions from fast exchange at concentrations higher than 50 mM does not create any inconsistencies when describing irradiated Fricke solution with the fast exchange model and its empirical parameters described above because the maximum ferric ion concentration in Fricke solution is 1 mM, well inside the linear portion of Fig. 10 for both ions.

The two site exchange model has been justified and it describes a solution of either ferrous or ferric ions quite well. In order to describe irradiated Fricke solution which contains both Fe^{2+} and Fe^{3+}

ions, however, it is necessary to extend the two site exchange model to three sites. In irradiated Fricke solution, protons on water molecules in the coordination shell of either ion are exchanging both with each other and with free protons not bound to either ion. The relaxation rate R_T of a solution containing both ions can thus be written:

$$R_T = p_b^{2+} R_{in}^{2+} + p_b^{3+} R_{in}^{3+} + (1 - p_b^{2+} - p_b^{3+}) R_w \ . \quad (4.13)$$

Again the bound fractions p_b^{2+} and p_b^{3+} are proportional to the concentration of ion in solution and the ionic concentration is low enough that there is no overlap of the hydration spheres. After some algebraic manipulations, Eq. (4.13) can be written:

$$R_T = f\ [Fe^{2+}] + g\ [Fe^{3+}] + R_w \ , \quad (4.14)$$

where f and g, as defined earlier, represent the ability of the respective ion to promote relaxation and are equal to the slopes of the lines in Fig. 10 for ferrous and ferric ion, respectively.

To verify whether the extension to the three site exchange model is valid for irradiated Fricke solution, the spin-lattice relaxation rates of solutions containing both ferrous and ferric ions at a total ionic concentration of 1 mM were determined, i.e., $[Fe^{2+}]$ and $[Fe^{3+}]$ individually varied but $[Fe^{2+}]+[Fe^{3+}]$ remained constant at 1 mM. This total ionic concentration was chosen because it mimics the total ionic concentration of Fricke solution. The results are shown in Fig. 11; the points are the measured relaxation rates and the line is the relaxation rate behaviour predicted by Eq. (4.14). The agreement

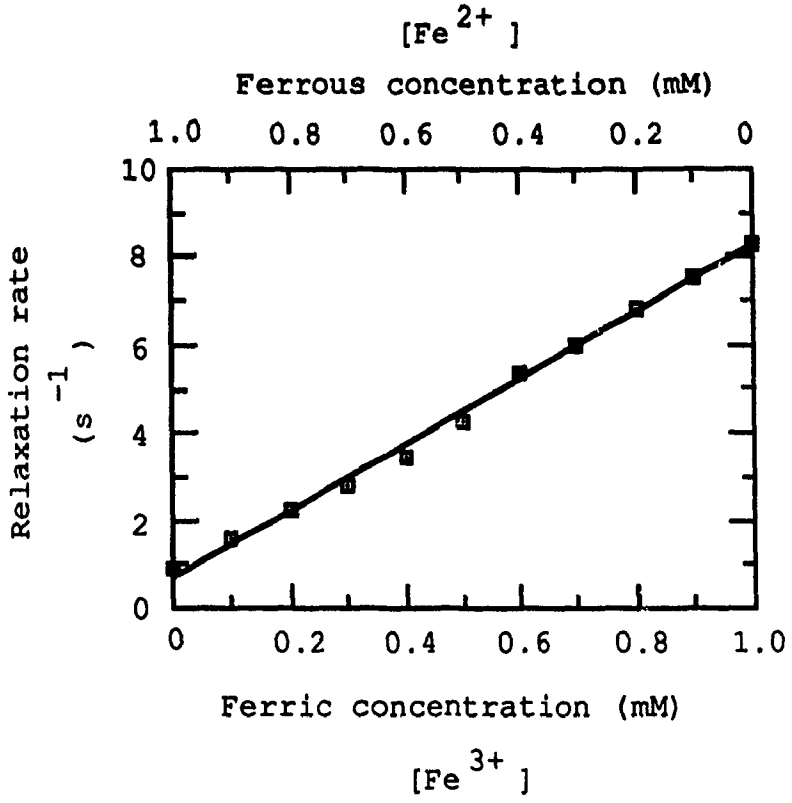

Figure 11 : The spin-lattice relaxation rate of a solution of ferric and ferrous ions (the total iron ionic concentration is constant at 1 mM) as a function of the ionic concentration. The solid line is calculated from the exchange model and the points are measured data. These data mimic the relaxation behaviour of irradiated Fricke solution

of the data with the three site fast exchange model is excellent. This experiment was repeated for solutions of ferrous and ferric ions including 1 mM NaCl and it was found that the chloride ion had no effect on the relaxation behavior. This is not unexpected since low concentrations of NaCl are known not to perturb R_w (Hertz, 1973); therefore the relaxation rate of a 1 mM NaCl solution does not differ from that of the bulk water. In extending the two site model describing the spin-lattice relaxation of individual ferrous and ferric solutions to the three site model describing the relaxation of the irradiated Fricke solution it is assumed that the two ions do not interfere with each other's hydration or their inherent relaxation. Therefore, the slope of the least squares fit to the data in Fig. 11 should be numerically equal to the difference of the constants f and g determined for the individual solutions. This is the case: $f = 0.45 \pm 0.01\ s^{-1}mM^{-1}$, $g = 7.98 \pm 0.08\ s^{-1}mM^{-1}$ and the slope of the line through the data points in Fig. 11 is $7.53 \pm 0.07\ s^{-1}mM^{-1}$. Hence the extension of the two site exchange model to the three sites in irradiated Fricke solution is valid.

The saturation value of the spin-lattice relaxation rate in Fig. 7 should be identical to the spin-lattice relaxation rate of a 1 mM solution of ferric (Fe^{3+}) ions in Fig. 11. This is not observed. The discrepancy results from the different oxygen concentrations in the Fricke mimicking solutions and the actual irradiated Fricke solution. While the Fricke mimicking solutions are all equally aerated, the irradiated Fricke solutions have a dissolved oxygen concentration which depends on the absorbed dose. As described above, oxygen is paramagnetic and enhances the spin-lattice relaxation of the solutions. Calculations using the data of Fig. 11

show that the enhancement caused by dissolved oxygen can be neglected in the linear region of Fig. 7 (dose < 250 Gy). The relaxation enhancement caused by the oxygen becomes more significant at greater doses, i.e., larger Fe^{3+} concentrations, because of the already short relaxation times of these solutions. While the relaxation behaviour of Fricke solutions irradiated to very high doses cannot be accurately predicted with the present model, the spin-lattice relaxation rates of Fricke solutions irradiated to doses below the saturation dose are well modelled. The oxygen effect can be neglected for the lower doses and it is possible to use the derived relaxation parameters to devise an absolute dosimetry system. Before this can be achieved, it is necessary to establish the chemical yield of ferric ion in irradiated Fricke solution.

4.3.2 Determination of the chemical yield

The three-site exchange model for the spin-lattice relaxation of aqueous solutions of ferrous and ferric ions can be used to determine the chemical yield of the Fricke solutions through Eq. (4.14). In the irradiated Fricke solutions the total iron ionic concentration (say q) remains constant independently of the dose absorbed during the irradiation, i.e., $[Fe^{2+}] + [Fe^{3+}] = q$ throughout the ionic evolution of the Fricke solution. Therefore, Eq. (4.14) can be written as:

$$R_T - R_W = fq - f\,[Fe^{3+}] + g\,[Fe^{3+}]. \qquad (4.15)$$

The relaxation rates R_T and R_w are those measured for the irradiated Fricke solutions and the bulk water, respectively; the f and g are determined from the spin relaxation measurements of the separate solutions of the ferrous and ferric ions and the q is set in the preparation of the Fricke solution (in this work q = 1 mM). Solving Eq. (4.15) for the concentration of ferric ion $[Fe^{3+}]$ gives:

$$[Fe^{3+}] = \left\{ \frac{R_T - R_w - fq}{g - f} \right\}. \qquad (4.16)$$

The chemical yield of the Fricke solution is defined to be the amount of ferric ion formed per energy absorbed by the dosimeter (ions per 100 eV). Since the energy absorbed is the absorbed dose multiplied by the mass of the solution, the chemical yield can also be given in terms of the following quantities used in this work: the molarity of the ferric ion and the absorbed dose. Equation (4.16) with the assumption that the ferric ion concentration was zero before irradiation gives:

$$G = \frac{1}{D} \left\{ \frac{R_T - R_w - fq}{g - f} \right\}, \qquad (4.17)$$

where D is the absorbed dose. Therefore, if the relaxation rate data for the irradiated Fricke solutions is plotted as $(R_T - R_w - fq)$ versus $(g - f)\,D$, the data should lie on a straight line with slope equal to the chemical yield G. Figure 12, based on the relaxation

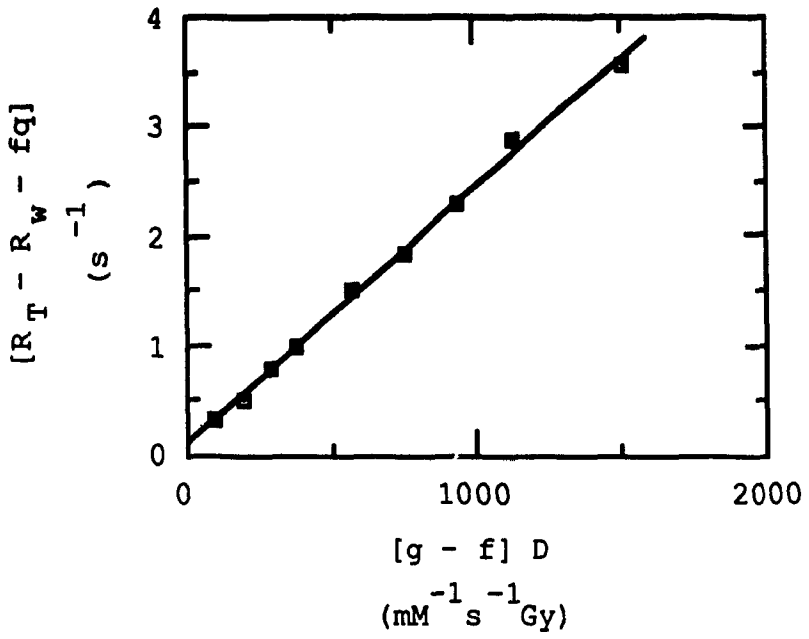

Figure 12 : Use of the three site exchange model to calculate the chemical yield G of ferric ion in Fricke solution. The ordinate and abscissa are essentially the relaxation rate and dose modified by the inherent relaxation parameters and concentration of ions (see text). The solid line is a least squares linear fit with a slope equal to G.

rates plotted in the linear region of Fig. 7 (recall that the saturation of the NMR dose response occurs at ~∠50 Gy), is such a plot and gives a chemical yield of (23.4 ± 0.6) x 10^{-7} M/Gy or, in more conventional units, G = 22.5 ± 0.6 ions/100 eV.

As the dose response curve for modified Fricke solution is known (see Fig. 7), the chemical yield can be calculated empirically since the relaxation rate dependence on the ferric ion concentration in the Fricke solution has also been determined in this work (see Fig. 11). A number of aqueous solutions containing different concentrations of ferrous and ferric ions but with a total ionic concentration fixed at 1 mM were prepared and their spin-lattice relaxation rates determined. As stated earlier, these solutions simulate the changes of ionic concentration in an irradiated Fricke solution. The relaxation rate increases linearly with increasing ferric concentration and the slope of the least squares fit of the data in Fig. 11 is 7.53 ± 0.07 $s^{-1}mM^{-1}$. The NMR sensitivity of the Fricke solution to radiation dose as determined from the data shown in Fig. 7 is 0.0182 ± 0.004 s^{-1} Gy^{-1}. The chemical yield for the Fricke solution is the ratio of these two slopes: empirically G = (24.2 ± 0.8) x 10^{-7} M/Gy (or, G = 23.3 ± 0.8 ferric ions per 100 eV). This value for the chemical yield is determined from measurements on solutions containing both ionic species and is in excellent agreement with the value (G = 22.5 ± 0.6 ions/100 eV) predicted by the three site exchange model with the constants f and g determined from separate solutions of either ion. This agreement is not unexpected since the spin-lattice relaxation of solutions containing both ferrous and ferric ions is accurately described by the three site exchange model (see Fig. 11). The slight discrepancy between the two

numerical values of G results from the fact that the determinations of G require the fitting of three independent sets of data.

Although the measurements described above give the chemical yield for the NMR Fricke dosimetry technique, they cannot be used to establish an absolute NMR Fricke dosimeter since the spin-lattice relaxation rate of an irradiated Fricke solution is not determined in terms of the basic NMR parameters of the solution. To establish an absolute NMR Fricke dosimetry system the spin-relaxation model for the Fricke solutions must be employed (see below).

The chemical yields determined by both methods above are equal within experimental error although they are significantly higher than the accepted value of 15.5 ions/100 eV (Attix et al., 1966). In practice, the chemical yield is very sensitive to the presence of impurities in the Fricke solution and to the volume of the irradiated dosimeter (see §4.6). Therefore, it is necessary to determine the chemical yield for the Fricke dosimeter preparation protocol established in a particular laboratory. However, as shown in this work, the reproducibility of the NMR Fricke dosimetry is excellent once the experimental technique is properly established and the chemical yield need only be determined once.

4.3.3 Absolute dosimetry formalism

Since all the inherent relaxation parameters describing the spin-lattice relaxation of a solution of ferrous and ferric ions are known, the NMR-Fricke dose measuring technique can be made absolute. Incorporating the definitions of the constants f and g in terms of

the inherent relaxation rates for the ferrous and ferric ions, R_{in}^{2+} and R_{in}^{3+} respectively, into Eq. (4.16) gives:

$$[Fe^{3+}] = \frac{R_T - \ell q\, R_{in}^{2+} - R_w\,(1-\ell q)}{\ell\,(R_{in}^{3+} - R_{in}^{2+})}\,, \qquad (4.18)$$

where ℓ is the proportionality constant between the fraction of bound water molecules and the ionic concentration for both ions and q is the total ionic concentration. The dose D absorbed by an irradiated Fricke solution is the ratio between the concentration of ferric ions produced by the radio-chemical oxidation of ferrous ions and the chemical yield for ferric ion ($[Fe^{3+}]/G$), therefore:

$$D = \frac{1}{G}\left\{\frac{R_T - \ell q\, R_{in}^{2+} - R_w\,(1-\ell q)}{\ell\,(R_{in}^{3+} - R_{in}^{2+})}\right\}\,. \qquad (4.19)$$

Since the chemical yield for the ferric ion has been established, Eq. (4.19) can be used to determine the dose absorbed by a Fricke solution directly from a measure of the solution's spin-lattice relaxation rate R_T.

The methodology used in deriving the spin-lattice relaxation model for irradiated Fricke solution can be used to determine either the absorbed dose, using Eq. (4.19), or the chemical yield, using Eq. (4.17). The chemical yield is best determined by experiments which do not depend explicitly on the spin exchange model for the spin-lattice relaxation. The method of determining G using the ratio of the NMR sensitivity and the dependence of the spin-relaxation rate of the Fricke mimicking solutions on the ferric ion concentration, described in §4.3.2 above, gives such a model independent

determination. That this empirical value of the chemical yield agrees with that predicted by the three site spin exchange model is a verification of the model. However, this value of the chemical yield for the NMR Fricke dosimetry technique alone cannot be used to establish an absolute NMR Fricke dosimeter since it does not relate the spin-lattice relaxation rate of an irradiated Fricke solution to the basic NMR parameters of the solution. The relationship between the relaxation rate of an irradiated Fricke solution and the ferric ion concentration is given by the three-site exchange model. Therefore using Eq. (4.19), based on the spin-relaxation model, with the chemical yield determined independently of any other dosimetry technique establishes an absolute dosimeter.

4.4 PRECISION OF THE NMR DOSIMETRY TECHNIQUE

One measure of the utility of any dosimetric technique is the lowest dose which can be accurately measured. The probing of chemical dosimeters is inherently less sensitive than that of ionization chambers or thermoluminescent materials and the NMR technique of measuring the dose response of Fricke solution is further limited by the accuracy of the measurement of the relevant NMR parameters. Analogously to the minimum detectable activity (ICRU, 1972), the minimum detectable dose can be defined as that dose which increases the spin-lattice relaxation rate of the Fricke dosimeter by an amount equal to three times the standard deviation in the relaxation rate of the unirradiated dosimeter (Olsson et al., 1989). Olsson et al. (1988) found a minimum detectable dose of 1 Gy

while Gore et al. (1984) claim that their system is capable of accurately measuring the changes in Fricke solution produced by an absorbed dose of 4 Gy. The zero dose precision in the relaxation time measurement with our present NMR spectrometer is 2 percent which limits the minimum detectable dose to 4 Gy. The dose resolution of the NMR-Fricke method, assuming a resolution of 0.01 s^{-1} in the spin-lattice relaxation rate measurement, is 0.5 Gy. With respect to other dosimetry techniques, the minimum detectable dose and the dose resolution of the NMR dosimetry system do not compare favourably for medical physics purposes. However, the three dimensional potential of the NMR Fricke method indicated by Gore et al. (1984), Hiraoka et al. (1986), Szeredi et al. (1986), and deGuzmann et al. (1989) motivates an investigation into the possibility of improving the minimum detectable dose and the dose resolution of the NMR dosimetry system. There are a number of ways by which the minimum measurable dose and the dose resolution of the NMR Fricke dosimetry technique can be improved. These are all based on the choice of the dosimeter itself and are independent of the spectrometer and any hardware used in the relaxation time measurements. One method of improving the NMR Fricke dosimetry technique, based on the addition of organic impurities to the Fricke solution, is addressed in the next section.

4.5 INCREASING THE SENSITIVITY OF FRICKE SOLUTION

It has been demonstrated that sensitizers such as benzoic acid (Balkwell and Adams, 1960) and ethanol (Dewhurst, 1952) have the ability to increase the chemical yield of ferric ion in Fricke solution (recall the discussion in Chapter 2). This has also been

observed in NMR studies of Fricke solutions containing organic gels (Gore et al., 1984b; Hiraoka et al., 1986; Appleby et al., 1987, 1988; Olsson et al., 1988). These latter studies were undertaken primarily to devise phantoms whose ionic distributions would be spatially stable and thereby could be used as a three dimensional MRI Fricke dosimetry technique. Hiraoka et al. (1986) have shown that the NMR sensitivity to radiation of the gelled Fricke dosimeter was greater than that of conventional aqueous Fricke solution. An increase in the NMR sensitivity to radiation of the dosimeter results in a lower minimum detectable dose and a better dose resolution and, in fact, Olsson et al. (1989) have found that the minimum detectable dose is a factor of approximately two lower in the gelled Fricke solution than in the aqueous solution. Appleby et al. (1987) have shown that the mechanism by which the sensitivity to radiation of Fricke solution doped with gels is increased is similar to that in solutions doped with other organic impurities.

To study the enhancement in the sensitivity of the Fricke dosimeter, modified Fricke solution was doped with varying concentrations of 100% ethanol (Consolidated Alcohol Limited, Toronto, Ontario). As a preliminary study, the dose responses of the Fricke solutions were determined. They were found to be linear to at least 100 Gy over the entire doping concentration range studied. It was also determined that the spin-lattice relaxation rate of unirradiated Fricke solution is not affected by the ethanol dopant. The linearity of the dose response curve along with the invariance in the unirradiated spin-lattice relaxation rate with increasing ethanol concentration imply that a full dose response curve is not needed in order to determine the sensitivity to radiation of a doped Fricke

solution. With this consideration, modified Fricke solution was doped with varying concentrations of 100% ethanol. The dosimeters were prepared independently four times and were subsequently irradiated to 50 Gy. Figure 13 shows a plot of the spin-lattice relaxation rate of each dosimeter as a function of the dopant concentration. The spin-relaxation rates for the irradiated solutions increase very quickly with ethanol concentration peaking at a concentration of ~0.02 M. The relaxation rate at the maximum is approximately 1.6 times the rate for the solution which was not doped. The ethanol dopant has the effect of increasing the amount of ferric ion which is produced by a fixed absorbed dose, in this case 50 Gy. This implies that the chemical yield of ferric ion increases with increasing ethanol dopant concentration up to 0.02 M. Similar behavior has been noted by Dewhurst (1952). There is a significant spread in the measured relaxation rates for the different dosimeters with doping concentrations less than 0.02 M. The spread cannot be explained by the measurement error associated with the NMR measurement procedure as undoped solution gives very reproducible results. The variation is probably the result of human error in the chemical doping of the solution; the likelihood of errors when working with very small concentrations of ethanol is increased. A lack of reproducibility has also been noted previously (Schulz, 1989). At higher doping concentrations the relaxation rates, and hence the chemical yields, are not maximized, however, the reproducibility of the results is better and the relaxation rate is much less sensitive to the concentration of ethanol. Therefore, ethanol concentrations in the range 0.05 M to 0.07 M should be added to the modified Fricke solution in order to increase the chemical yield of the dosimeter reproducibly. In this range of ethanol

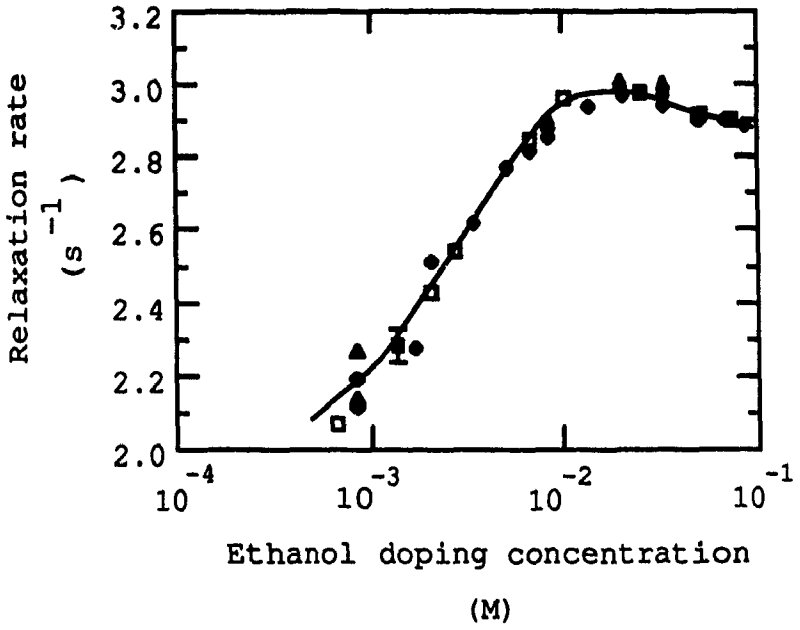

Figure 13 : The spin-lattice relaxation rate of a modified Fricke solution as a function of ethanol doping concentration. Different symbols represent data from different dosimeter preparations. The line is not a fit but an aid to the eye. A representative error bar is indicated.

concentrations the sensitivity of Fricke solution is increased by a factor of ~1.5.

Similar experiments were also performed with standard Fricke solutions containing no NaCl: even higher sensitivities were achieved. However, the spin-lattice relaxation rates measured for different solutions doped to the same ethanol concentration and irradiated to the same dose were not reproducible. This is expected since the chloride ion is not available to stabilize the Fricke reactions (see Chapter 2). Attempts to increase the chemical yield of standard Fricke solutions (without NaCl) by doping them with organic impurities are not practical.

4.6 VOLUME OF IRRADIATED SOLUTION AND ITS RELATION TO NMR SENSITIVITY

The NMR sensitivity of the Fricke solution determined in this laboratory (0.0182 ± 0.0004 s^{-1} Gy^{-1}) is in excellent agreement with that reported by Szeredi et al. (1986) and Olsson et al. (1989). This sensitivity corresponds to a ferric ion chemical yield of ~23 ions per 100 eV, higher than the accepted value of 15.5 ions per 100 eV (Attix et al., 1966). Gore et al. (1984), however, have published a Fricke NMR sensitivity of 0.0113 ± 0.0002 s^{-1} Gy^{-1} corresponding to a ferric ion chemical yield of 15 ferric ions per 100 eV of absorbed energy, in close agreement with the accepted value. The discrepancies between the published sensitivities may result from a number of factors. As indicated in §3.2 and §4.5, organic impurities may elevate the chemical yield of ferric ion in Fricke solution.

Therefore, for absolute dosimetry it is essential that every component of the Fricke dosimeter (the chemicals and the glass containers utilized in the dosimeter preparation and storage and the dosimeter cells used for the dosimeter irradiation) be free of macroscopic and microscopic impurities. It is expected that all the workers discussed above used equally good chemical techniques and macroscopic cleaning protocols. Variations in glassware cleaning procedures and in the concentration and type of organic impurity which may contaminate different glass make the assessment of the removal of microscopic impurities by different laboratories more difficult. For example, it has been reported that it is possible to remove the microscopic organic impurities by pre-heating the dosimeter cells (Attix et al., 1966), however, this procedure showed no effect on the NMR sensitivity and chemical yield of the Fricke dosimeter used in these experiments (see Chapter 3). Also, some microscopic impurities which infiltrate the glassware are released only during irradiation (Hart and Matheson, 1952; Armstrong et al., 1963). These contaminants can be removed by pre-irradiating the dosimeter cells to about 10^5 Gy (Attix et al., 1966); at the dose rates typically available in the clinical setting month long irradiations are required for this cleaning. Therefore, pre-irradiation of the dosimeter cells has not been performed in this work. None of the other groups mentioned above describe explicitly their particular microsopic cleaning protocols nor do they specify the type of glassware used. This makes a comparison of the different reported NMR sensitivities (and associated chemical yields) based on an assessment of the removal of microscopic impurities even more difficult.

The only recognizable difference between the techniques used in our laboratory and those employed by any of the other research groups is the volume of dosimeter which is irradiated. In this work the volume of irradiated Fricke solution was 68 μL while Gore et al. irradiated 1 mL of solution; Szeredi et al. (1986) and Olsson et al. (1989) do not quote the volume of their dosimeter cells. The different NMR sensitivities reported for the different dosimeter volumes suggest that there is a relationship between the volume of Fricke solution irradiated and its NMR sensitivity. To study this relationship modified Fricke solution was irradiated in samples of both 68 μL and 10000 μL volumes; all glassware was cleaned identically according to the protocol outlined in Chapter 3. The glass cells in which the solutions were irradiated were composed of similar quality and type of glass. For the NMR spin-lattice relaxation measurement of the Fricke solution irradiated in the larger dosimeter cells, 68 μL of the solution from the cell was transferred into an NMR sample tube. The resulting spin-lattice relaxation data are shown in Fig. 14. The NMR sensitivity of the larger volume of Fricke solution was 0.0146 ± 0.0003 s^{-1} Gy^{-1} ($G = 18.6 \pm 0.4$ ions/100 eV), which is ~25 percent lower than that of the 68 μL sample. The increase in chemical yields for the Fricke solutions irradiated in the two different volumes with respect to the accepted value is considered to result from organic impurities in the dosimeter cell walls which are released by the irradiation. Both dosimeters have enhanced NMR sensitivities and chemical yields, although the enhancement for the larger volume dosimeter is less pronounced. This is expected since the ratio between the surface area of the dosimeter cell in contact with Fricke solution and the

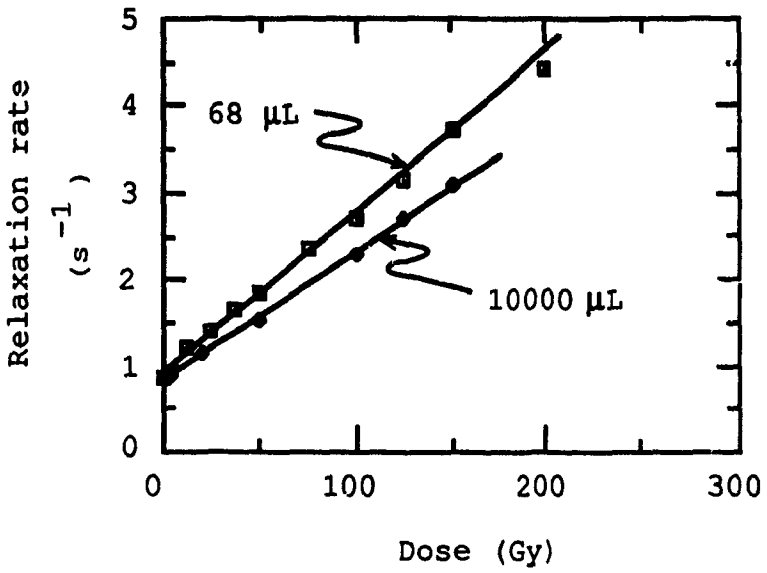

Figure 14 : Dose response of the spin-lattice relaxation rate of Fricke solution irradiated in dosimeter cells with volumes of 68 µL and 10000 µL. The solid lines are least square fits of the data from which the NMR sensitivities of the dosimeters can be determined: 0.0182 and 0.0146 $s^{-1}\,Gy^{-1}$ for the 68 µL and 10000 µL samples respectively.

solution volume is different for the two dosimeters: the ratios are ~1 mm^{-1} and ~0.23 mm^{-1} for the 68 µL and 10000 µL dosimeters, respectively. Since the impurities originate in the cell walls, these ratios imply that the relative impurity concentration is higher in the smaller volume dosimeter than in the larger one. It is interesting to note that the dosimeter in the experiments performed by Gore et al. (1984) had a volume of 1000 µL, which is between the two volumes irradiated in this work, yet the NMR sensitivity for his dosimeter corresponds to the accepted ferric ion chemical yield. This may be explained if Gore et al. (1984) used irradiation cells that were infiltrated by a lower number of microscopic impurities, if their cells had a different geometry with a surface area to volume ratio lower than that of this work, or if the dosimetry cells were pre-irradiated. Unfortunately, these experimental details were not reported.

This preliminary work suggests that there is a relationship between the ratio of the surface area to volume for the irradiated dosimeter and its NMR sensitivity. The enhancement of the ferric ion chemical yield seems to result from organic impurities which are released from the dosimeter cell wall during the irradiation. Two previous experiments corroborate this explanation. The sensitivity of modified and standard Fricke solutions differ implying that organic impurities are present in the Fricke solutions. From this experiment alone one cannot conclude whether the impurities are introduced during the Fricke solution preparation or during the irradiation of the dosimeter. To investigate the source of the impurities, further experiments were performed on modified Fricke solution prepared at the National Research Council (NRC) in Ottawa,

Canada, where, since the NRC is a standardization laboratory, stricter dosimeter preparation protocols are used. The dosimeters were irradiated in the dosimeter cells from our laboratory. The NMR senstivity was identical to that for Fricke dosimeters prepared by the author. This suggests that the cleaning protocol established in this laboratory is sufficient to remove any macroscopic impurities from the dosimeter and the chemicals used in the dosimeter preparation are adequately pure. Impurities which infiltrate the solution arise from the dosimeter cell wall. This presents a problem if an absolute dosimetry system is to be established because the type and concentration of impurity in the dosimeter cell wall is inherently dependent on the particular type of glass which comprises the cell wall. However, the elevated NMR sensitivity is highly reproducible and has been reported by other groups (Szeredi et al., 1986; Olsson et al., 1989). It also results in a dosimeter with an improved minimum detectable dose and dose resolution. Therefore, from the point of view of practical absolute dosimetry, it is not necessary to remove the microscopic impurities from the dosimeter cell wall since the chemical yield, although different from the accepted value, is constant at ~23 ions/100 eV. The reproducibility of the elevated chemical yields obtained by different research groups casts some suspicion on the conclusion that the effect results solely from contamination with impurities originating in the dosimeter cell wall. It is possible that varying interface effects at the cell wall for different irradiation geometries cause the differences in the chemical yields implied in Fig. 14. New experiments are being undertaken to improve the understanding of the source of the elevated sensitivity and its implication for the NMR Fricke dosimetry technique.

4.7 RATIONALE FOR USING 1 mM FERROUS ION IN FRICKE SOLUTION

The standard and modified Fricke solutions are prepared with a 1mM initial ferrous ion concentration. Historically, this concentration was chosen so that the ionic solution had the same mass absorption coefficient for x rays as does air (Fricke and Petersen, 1927). In this section an analysis of the spin-lattice relaxation data for aqueous solutions with different concentrations of ferrous and ferric ions is outlined. The analysis supports the choice of an initial ferrous ion concentration of 1 mM for a practical NMR dosimetry technique.

The most precise measure of dose is obtained from a dosimeter whose response is greatly affected by the irradiation. In NMR Fricke dosimetry, the response is the spin-lattice relaxation time of the Fricke solution, hence a large response implies a large difference in the T_1's measured before and after the irradiation. Although not intuitively clear, it can be shown that the NMR response is dependent on the initial ferrous concentration in the Fricke solution. The total iron ionic concentration q in a Fricke dosimeter is equal to the initial ferrous ion concentration used in the preparation of the solution. The q remains constant throughout the history of the dosimeter; after the dosimeter absorbs a dose D, a certain concentration of the ferrous ions $[Fe^{2+}]$ is oxidized to ferric ions $[Fe^{3+}]$, but $[Fe^{2+}] + [Fe^{3+}] = q$. The spin-lattice relaxation rate for a solution containing ferrous and ferric ions in concentrations of $[Fe^{2+}]$ and $[Fe^{3+}]$, respectively, is given by Eq. (4.14). The

measured spin-lattice relaxation time is the inverse of the rate: $T_1 = 1/R_T$. Before irradiation, the total iron ionic concentration of the Fricke solution is $q = [Fe^{2+}]$ and the T_1 is:

$$T_1 = \frac{1}{fq + R_w} . \tag{4.20}$$

The T_1 of the solution after irradiation is:

$$T_1 = \frac{1}{f\,(q - [Fe^{3+}]) + g\,[Fe^{3+}] + R_w} . \tag{4.21}$$

As defined in §4.3, the f and g are dependent on the inherent relaxation rates of the protons on water molecules in the coordination shells of the ferrous and ferric ions, respectively, and the R_w is the spin-lattice relaxation rate of the bulk water protons. The response of the dosimeter is the change in the measured spin-lattice relaxation time before and after irradiation, ΔT_1 (the difference between Eq. (4.20) and Eq. (4.21)). The ferric ion concentration after irradiation is equal to the absorbed dose D multiplied by the chemical yield G; i.e., $[Fe^{3+}] = DG$. Therefore, the NMR response is dependent on the concentration of ferric ions formed by the irradiation and on the total iron ionic concentration q in the dosimeter. Also, although the chemical yield of the Fricke solution is independent of q (Krenz and Dewhurst, 1949), the response of the dosimeter varies with q. The initial concentration q which gives the optimum response of the Fricke solution can be determined by maximizing the rate of change of the response with respect to the ferric concentration since $d\Delta T_1/dD = (1/G)\, d\Delta T_1/d[Fe^{3+}]$. From the

difference of Eqs. (4.20) and (4.21), the rate of change, $d\Delta T_1/d[Fe^{3+}]$, is:

$$\frac{d\Delta T_1}{d[Fe^{3+}]} = \frac{(g-f)}{\{fq + (g-f)\,[Fe^{3+}] + R_w\}^2} \,. \qquad (4.22)$$

This quantity is plotted as a function of q in curve (a) of Fig. 15. There is an inverse relationship between the dosimeter response resulting from the production of a given ferric concentration and the total ionic concentration q. For a given dose, the dosimeters with the smallest q have the largest responses. This is expected since even though a dose D will produce an identical ferric concentration irrespective of q, lower values of q will result in a greater dosimeter response. For a very high q, the relative number of ferric ions is small and the perturbation in T_1 resulting from the radiation created ferric concentration is minimal. In terms of the NMR measurement technique, it is desirable to maximize the relative response in order to reduce the relative error. With this consideration alone, curve (a) in Fig. 15 suggests that Fricke solutions with lower initial ferrous concentrations are better dosimeters since they have larger responses. However, the relationship between the total ionic concentration and the saturation dose for that q is also important (curve (b) in Fig. 15). When the initial ferrous ion concentration in the Fricke solution is low, saturation of the ferric ion concentration and of the NMR response occurs at lower doses and the system becomes unreliable. This has been noted by Olsson et al. (1988) for a Fricke solution prepared with 0.01 mM ferrous ion. It is necessary to make a compromise

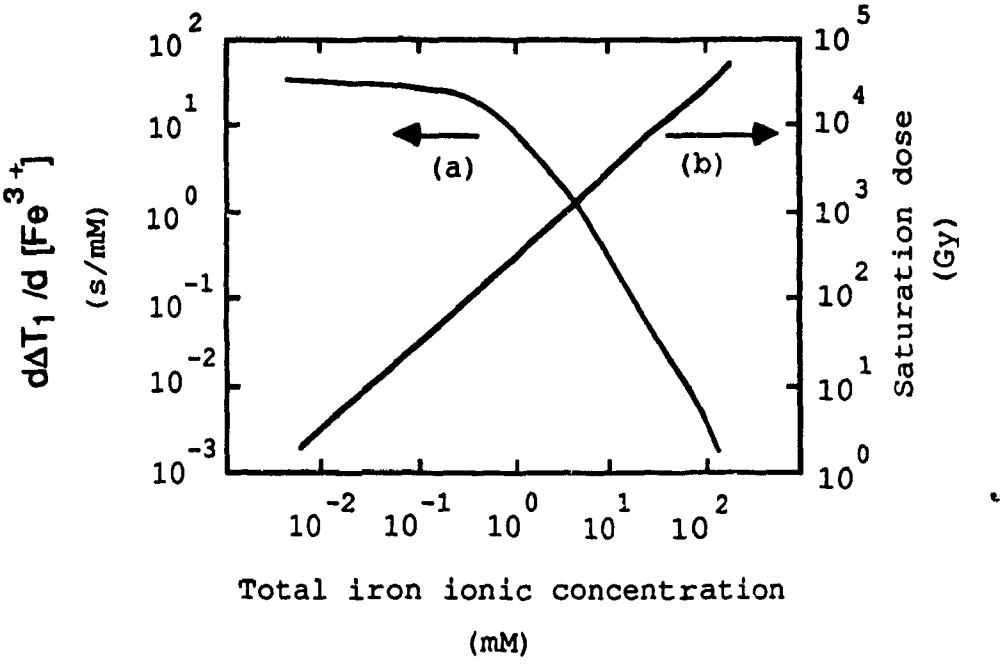

Figure 15 : (a) The rate of change of the Fricke dosimeter response as a function of the total iron ionic concentration q determined from the three site fast exchange model. (b) The theoretical saturation dose of the Fricke dosimeter as a function of q.

between dosimeters with high responses or those with high saturation doses. The conventional choice of 1 mM for the initial ferrous concentration is a good compromise, from both dosimetric and NMR considerations.

CHAPTER 5

CONCLUSIONS

The motivation for the experiments performed in this thesis was to study the physical processes which determine the NMR spin-relaxation of Fricke solution exposed to Co-60 radiation. Historically, spectrophotometry has been used to determine the relative proportion of ferrous and ferric ions in irradiated Fricke solution (Scharf and Lee, 1962), however, NMR has recently been proposed as an alternative probe (Gore et al., 1984). It was found that there is a linear relationship between the spin-lattice relaxation rate of irradiated modified Fricke solution and the absorbed dose up to a dose of about 250 Gy. For higher doses, the response is no longer linear and at doses higher than ~270 Gy the response of the Fricke dosimeter saturated.

The reproducibility of the NMR spin-lattice relaxation rate measurements was studied. It was determined that unless very precise protocols are used in the preparation of the Fricke solution (including the cleaning of all glassware), the reproducibility of the dose response is not adequate. The problem does not result from inaccuracies in the NMR measurements, but arises from variations in the Fricke solution chemistry which may alter the dose response of the dosimeter. Once the dosimeter preparation protocols described in this thesis were implemented, the Fricke solution was no longer a variable in the experiments. Any subsequent variability in the

measurement of the dose response, although minimal in these experiments, would result from the precision of the NMR system.

In developing a model for the spin-lattice relaxation behaviour of irradiated Fricke solution containing both ferrous and ferric ions, the behaviour of a spin system consisting of separate aqueous solutions of either ion was first investigated. A model based on fast exchange between protons on bulk water molecules and those on water molecules in the coordination shell of an ion was proposed and experimentally verified. This model was then extended to irradiated Fricke solution by considering three spin groups: protons on bulk water molecules exchanging with protons on water molecules bound to either a ferrous or ferric ion. Gore et al. (1984) have mathematically characterized the relaxation behavior of irradiated Fricke solution, although the inherent spin-lattice relaxation rates of protons on water molecules in the coordination shell of an ion were not quantified. In deriving the model for this thesis, many of the published inherent parameters (Gore et al., 1984) describing the spin-lattice relaxation of ferrous and ferric ionic solutions were reproduced and the inherent relaxation rates for protons on water molecules in the coordination shell of an ion were quantified for the first time. This quantification of the inherent relaxation rates allows the extension of the NMR dosimetry technique to an absolute dosimetry, provided that the chemical yield of the ferric ion is well established. The model also allows one to predict the NMR dose response of a Fricke dosimeter which is prepared using a non-standard recipe. An example of this use of the model is presented in this

thesis: a theoretical justification of the use of 1 mM initial ferrous concentration in the preparation of Fricke solution is described.

The NMR sensitivity of the Fricke dosimeter determined in this thesis was identical to that reported by Olsson et al. (1989) and Szeredi et al. (1986), although it was appreciably higher than that given by Gore et al. (1984). This implies that there are variations in the chemical yields for the Fricke dosimeter. If the NMR technique is to be established as an absolute dosimetry system, the chemical yield must be constant, or the reasons for variations in the yield must be well understood. Since it is expected that the Fricke solution preparation protocols used in the different laboratories were equally good, the differences in chemical yields must be the result of some other factor. A possible explanation for the discrepancy in chemical yields is proposed in this thesis. It is based on an irradiation-induced release of microscopic organic impurities from the dosimeter cell wall. The magnitude of the effect appears to be related to the ratio between the surface area of the Fricke solution in contact with the dosimeter cell wall and the volume of the solution itself. Although only preliminary studies have been described in this thesis, future work in this laboratory will involve a more complete characterization of the physical processes which govern the effect.

One measure of the usefulness of any dosimetric tool is the lowest dose which can be accurately measured. As described above, the NMR technique of measuring the dose response of Fricke solution

is limited by the precision of the NMR measurements. Gore et al. (1984) claim that their system is capable of accurately resolving the changes in Fricke solution produced by an absorbed dose of 4 Gy while Olsson et al. (1988) found a minimum detectable dose of 1 Gy. The minimum measurable dose for the dosimeter used in this thesis was 4Gy with a dose resolution of 0.5 Gy. For comparison, the spectrophotometric method of determining ferric concentration in Fricke solution has a minimum detectable dose of 0.08 Gy (Mattson et al., 1982). Therefore, in comparison to the stardard method of measuring the dose response of a Fricke dosimeter, the NMR method is relatively insensitive. There are a number of ways in which the minimum measurable dose and the dose resolution can be improved. If the NMR sensitivity of the Fricke solution can be increased, such as with the addition of organic impurities, the minimum measurable dose will be lower than that of undoped solution and the dose resolution will be improved. Fricke solution doped with ethanol was extensively studied in this thesis. It was found that the sensitivity of the solution increased with increasing concentration of ethanol, as expected, however, above a dopant concentration of 0.02 M the sensitivity slightly decreased. It is suggested that to increase the sensitivity of a Fricke dosimeter reproducibly, ethanol in concentrations of 0.05 M to 0.07 M should be added to the dosimeter. Ethanol dopant in this concentration range increases the NMR sensitivity and reduces the minimum detectable dose of the Fricke dosimeter by a factor of ~1.5.

In the process of conducting the research described in this thesis, an NMR laboratory consisting of a 25 MHz spectrometer and an electromagnet has been established at the Montreal General Hospital. Strict protocols for the preparation of Fricke solution were

determined. Future work in the NMR laboratory will involve the improvement of the accuracy of the NMR-Fricke technique by studying the responses of different dosimeter materials. Many of the techniques developed in this thesis will be utilized to characterize the dose responses of these new dosimeters.

APPENDIX

The following discussion shows the detailed calculation of the probability for transitions between the eigenstates of the spin operators. To illustrate the procedure, the intramolecular relaxation mechanism driven by isotropic reorientation of the water molecules associated with Brownian motion is derived. As described in Chapter 1, the major contribution to the spin-lattice relaxation is from the dipole-dipole interaction. The total Hamiltonian of a spin system comprised of two spins **I** and **S** coupled by the dipole-dipole interaction is given by Eq. (1.3), with the perturbation term $\mathcal{H}'$ given by Eq. (1.5). This perturbing Hamiltonian can be written in the following form (Solomon, 1955):

$$\mathcal{H}' = \left[I_z S_z - \frac{1}{4}(I_+ S_- + I_- S_+) \right] F_o + (I_+ S_z + I_z S_+) F_1 + \\ + (I_- S_z + I_z S_-) F_1^* + I_+ S_+ F_2 + I_- S_- F_2^* \,. \quad (A.1)$$

The raising and lowering operators I_+ and I_- are defined as:

$$I_+ = I_x + i\, I_y \quad (A.2)$$

$$I_- = I_x - i\, I_y \,, \quad (A.3)$$

and similarly for S_+ and S_-. The $F_j(t)$ are the Fourier spectra of the position coordinates for a spin located at (r, θ, φ) with the origin at the other spin in the water molecule. The molecule is considered rigid and the motion which governs the interproton vector is molecular tumbling. Therefore the interproton distance r is fixed

and only the angle coordinates of the interproton vector are variable in time. The $F_j(t)$ are thus given by (Bloembergen et al., 1948):

$$F_o(t) = k\,[1-3\cos^2\theta(t)] \qquad (A.4)$$

$$F_1(t) = -\frac{3}{2}k\,\sin\theta(t)\,\cos\theta(t)\,e^{i\varphi(t)} \qquad (A.5)$$

$$F_2(t) = -\frac{3}{4}k\,\sin^2\theta(t)\,e^{2i\varphi(t)}, \qquad (A.6)$$

with $k = \hbar^2\gamma_I\gamma_S/r^3$.

The functions given by Eqs. (A.4-A.6) will vary randomly with time because of the molecular reorientation. The motion is isotropic hence the time average of the functions $F_j(t)$ will be zero. Since the motion of the spins is statistical in character, we can define a correlation function of $F_j(t)$ given by:

$$\langle F_j(t)\;F_j^*(t+\tau)\rangle_{av} = K_j(t). \qquad (A.7)$$

The $K_j(t)$ contains information about the correlation between the positions of the spins at different times. The correlation function is assumed to be an even function of τ and to be independent of t (the tumbling is a stationary random process). It is given by the following relation (Bloembergen et al., 1948)

$$K_j(t) = \langle F_j(t)F_j^*(t)\rangle_{av}\,e^{-|\tau|/\tau_c} = \\ = \langle|F_j(0)|^2\rangle e^{-|\tau|/\tau_c}\ . \qquad (A.8)$$

A statistical average over the spatial coordinates of the Fourier spectra gives (Bloembergen et al., 1948):

$$\langle |F_0|^2 \rangle = \frac{4}{5} k^2 \qquad \text{(A.9)}$$

$$\langle |F_1|^2 \rangle = \frac{3}{10} k^2 \qquad \text{(A.10)}$$

$$\langle |F_2|^2 \rangle = \frac{3}{10} k^2, \qquad \text{(A.11)}$$

with k as defined above.

The transition probabilities can then be calculated using the formalism which was introduced in Chapter 1. Equation (1.6) includes the matrix element $\langle m_j | \mathcal{H}' | m_i \rangle$ which must be calculated for each transition. As an example the explicit calculation will be shown for w_1 which is the probability for a transition from |->|+) to |+>|+). Introducing the condensed notation

$$\langle\, |+>|+)\ \ |\mathcal{H}'|\ \ |->|+)\ \rangle \Rightarrow \langle ++|\mathcal{H}'|-+\rangle, \qquad \text{(A.12)}$$

leads (with the Hamiltonian $\mathcal{H}'$ given in Eq. (A.1)) to matrix elements of the form:

$$\langle ++|\ [I_zS_z-(I_+S_-+I_-S_+)]F_0/4 + [I_+S_z+I_zS_+]F_1 +$$

$$+ [I_-S_z+I_zS_-]F_1^* + I_+S_+F_2 + I_-S_-F_2^*\ |-+\rangle. \qquad \text{(A.13)}$$

The spin states are orthonormal and from the definition of the raising and lowering operators (Eqs. A.1 and A.2) the only nonzero term in (A.13) is $\langle ++|\ I_+S_z\ |-+\rangle$. The probability for a transition from |->|+) to |+>|+) is therefore:

$$w_1 = \frac{1}{t\hbar^2} \left| \int_o^t \frac{1}{2} F_1(t') \, e^{-i\omega_I t'} \, dt' \right|^2. \qquad (A.14)$$

Similar expansions can be made for the other transitions shown in Fig. 1 thereby giving the following transition probabilities

$$w_o = \frac{1}{t\hbar^2} \left| \int_o^t \frac{1}{4} F_o(t') \, e^{-i(\omega_I - \omega_S)t'} \, dt' \right|^2 \qquad (A.15)$$

$$w_1' = \frac{1}{t\hbar^2} \left| \int_o^t \frac{1}{2} F_1(t') \, e^{-i\omega_S t'} \, dt' \right|^2 \qquad (A.16)$$

$$w_2 = \frac{1}{t\hbar^2} \left| \int_o^t \frac{1}{2} F_2(t') \, e^{-i(\omega_I + \omega_S)t'} \, dt' \right|^2. \qquad (A.17)$$

Before the integrations in Eqs.(A.14-A.17) are performed, it is useful to distinguish between the two cases described in Chapter 1.

(a) **LIKE SPINS:** For the case of two identical spins, $\gamma_I = \gamma_S = \gamma$, $\omega_I = \omega_S = \omega_0$, and the integrals reduce to (Solomon, 1955)

$$w_o = \frac{\tau_c}{8\hbar^2} \langle |F_o|^2 \rangle \qquad (A.18)$$

$$w_1 = w_1' = \frac{\tau_c}{2\hbar^2} \langle |F_1|^2 \rangle \frac{1}{1+\omega^2\tau_c^2} \qquad (A.19)$$

$$w_2 = \frac{2\tau_c}{\hbar^2} \langle |F_2|^2 \rangle \frac{1}{1+4\omega^2\tau_c^2} \, . \qquad (A.20)$$

The values of the averages of the Fourier spectra (Eqs. A.9-A.11) can now be substituted into Eqs.(A.18-A.20) to give the probabilities for transitions between spin eigenstates in a system of identical spins:

$$w_o = \frac{1}{10}\frac{\hbar^2\gamma^4}{r^6}\,\tau_c \tag{A.21}$$

$$w_1 = w_1' = \frac{3}{20}\frac{\hbar^2\gamma^4}{r^6}\,\frac{\tau_c}{1+\omega^2\tau_c^2} \tag{A.22}$$

$$w_2 = \frac{3}{20}\frac{\hbar^2\gamma^4}{r^6}\,\frac{4\tau_c}{1+4\omega^2\tau_c^2}\,. \tag{A.23}$$

These transition probabilities can be substituted into Eq. (1.14) to obtain a relation for the spin-lattice relaxation time for a system of identical spins.

(b) **UNLIKE SPINS** : For the case of a system which is comprised of spins of two types (gyromagnetic ratios γ_I and γ_S), Eqs. (A.14-A.17) give the following relations for the probability of transitions between eigenstates of the spins in the system:

$$w_o = \frac{\tau_c}{8\hbar^2}\,\langle|F_o|^2\rangle\,\frac{1}{1+(\omega_I-\omega_S)^2\tau_c^2} \tag{A.24}$$

$$w_1 = \frac{\tau_c}{2\hbar^2}\,\langle|F_1|^2\rangle\,\frac{1}{1+\omega_I^2\tau_c^2} \tag{A.25}$$

$$w_1' = \frac{\tau_c}{2\hbar^2}\,\langle|F_1|^2\rangle\,\frac{1}{1+\omega_S^2\tau_c^2} \tag{A.26}$$

$$w_2 = \frac{2\tau_c}{\hbar^2}\,\langle|F_2|^2\rangle\,\frac{1}{1+(\omega_I+\omega_S)^2\tau_c^2}\,. \tag{A.27}$$

Inserting the values of the averages of the Fourier spectra given in Eqs. (A.9-A.11) into Eqs. (A.24-A.27) gives the following values for the transition probabilities:

$$w_o = \frac{1}{10}\frac{\hbar^2\gamma_I^2\gamma_S^2}{r^6}\frac{\tau_c}{1+(\omega_I-\omega_S)^2\tau_c^2} \tag{A.28}$$

$$w_1 = \frac{3}{20}\frac{\hbar^2\gamma_I^2\gamma_S^2}{r^6}\frac{\tau_c}{1+\omega_I^2\tau_c^2} \tag{A.29}$$

$$w_1' = \frac{3}{20}\frac{\hbar^2\gamma_I^2\gamma_S^2}{r^6}\frac{\tau_c}{1+\omega_S^2\tau_c^2} \tag{A.30}$$

$$w_2 = \frac{6}{10}\frac{\hbar^2\gamma_I^2\gamma_S^2}{r^6}\frac{\tau_c}{1+(\omega_I+\omega_S)^2\tau_c^2} \; . \tag{A.31}$$

A relation for the spin-lattice relaxation time for an aqueous solution of paramagnetic ions can be obtained by substituting the transition probabilities given in Eqs. (A.28-A.31) into Eq. (1.17).

REFERENCES

Abragam, A., 1961, **The Principles of Nuclear Magnetism**, Clarendon Press, Oxford, England.

Ahrens, R.W., 1967, **Gamma radiolysis of aqueous solutions containing Fe(II) and selected substituted phenols**, Radiat. Res. **30**, 611-619.

Allen, A.O., 1961, **The Radiation Chemistry of Water and Aqueous Solutions**, Van Nostrand, Princeton, New Jersey.

Appleby, A., Christman, E.A., and Leghrouz, A., 1987, **Imaging of spatial radiation dose distribution in agarose gels using magnetic resonance**, Med. Phys. **14**, 382-384.

Appleby, A., Leghrouz, A., and Christman, E.A., 1988, **Radiation chemical and magnetic resonance studies of aqueous agarose gels containing ferrous ions**, Radiat. Phys. Chem. **32**, 241-244.

Armstrong, W.A., Facey, R.A., Grant, D.W., and Humphreys, W.G., 1963, **A redetermination of the salicylic acid yield in the aqueous calcium benzoate dosimeter**, Radiation Res. **19**, 120-128.

Attix, F.H., Roesch, W.C., and Tochilin, E., eds., 1966, **Radiation Dosimetry**, vol. 2., 2nd ed.,Academic Press, New York, New York.

Balkwell, W.R. and Adams, G.D., 1960, **On the radiation chemistry of ferrous sulfate - benzoic acid dosimeter**, Radiation Res. **12**, 419-420 (abstract).

Barr, N.F. and Schuler, R.H., 1957, **The dependence of radiation chemical yields on rate of energy loss; the yields of molecular and radical products from 0.8 N sulfuric acid solutions**, Radiation Res. **7**, 302-303 (abstract).

Basson, R.A. and DuPlessis, T.A., 1967, **The influence of ethylene on the radiolytic oxidation of ferrous sulfate**, J. Chem Soc. A, 779-781.

Bevington, P.R., 1969, **Data Reduction and Error Analysis for the Physical Sciences**, McGraw-Hill, New York, New York.

Bloembergen, N., 1956, **Proton relaxation times in paramagnetic solutions**, J. Chem. Phys. **27**, 572-573.

Bloembergen, N. and Morgan, L.O., 1961, **Proton relaxation times in paramagnetic solutions. Effects of electron spin relaxation**, J. Chem. Phys. **34**, 842-850.

Bloembergen, N., Purcell, E.M., and Pound, R.V., 1948, **Relaxation effects in nuclear magnetic resonance absorption**, Phys. Rev. **73**, 679-712.

Cameron, J.R., Suntharalingam, N., and Kenney, G.N., 1968, **Thermoluminescent Dosimetry**, University of Wisconsin Press, Madison, Wisconsin.

Cottens, E., Janssens, A., Eggermont, G., and Buysse, J., 1982, **Study of the effect of chloride ion on the ferric ion yield of the Fricke dosemeter in the absence of impurities**, Phys. Med. Biol. **27**, 597-602.

Cotton, F.A. and Wilkinson, G., 1966, **Advanced Inorganic Chemistry: A Comprehensive Textbook**, Wiley, New York, New York.

Davies, J.V. and Law, J., 1963, **Practical aspects of ferrous sulfate dosimetry**, Phys. Med. Biol. **8**, 91-96.

deGuzman, A., Gore, J., and Schulz, R.J., 1989, **Dose response curves for gels infused with Fricke dosimeter by NMR**, Med. Phys. **16**, 457 (abstract).

Deverell, C., 1969, **Nuclear magnetic resonance studies of electrolyte solutions.** in **Progress in NMR Spectroscopy**, vol. 4, 235-334, (Emsley, J.W., Feeney, J., Sutcliffe, L.H., eds.), Pergammon Press, Oxford, England.

Dewhurst, H.A., 1952, **Effect of aliphatic alcohols on the γ-ray oxidation of aerated aqueous ferrous sulfate,** Trans. Farad. Soc. **48**, 905-911.

Dwek, R.A., 1975, **Nuclear Magnetic Resonance in Biochemistry: Applications to Enzyme Systems**, Clarendon Press, Oxford, England.

Dyne, P.J. and Kennedy, J.M., 1958, **Kinetics of radical reactions in the tracks of fast electrons. A detailed study of the Samuel-Magee method for the radiation chemistry of water**, Can. J. Chem. **36**, 1518-1536.

Edzes, H.T. and Samulski, E.T., 1978, **The measurement of cross-relaxation effects in the proton NMR spin-lattice relaxation of water in biological systems: hydrated collagen and muscle**, J. Magn. Reson. **31**, 207-229.

Eisinger, J., Schulman, R.G., and Szymanski, B.M., 1961, **Transition metal binding in DNA solutions**, J. Chem. Phys. **36**, 1721-1729.

Ellis, S.C., 1974, **The dissemination of absorbed dose standards by chemical dosimetry - mechanism and use of the Fricke dosemeter**, Rad. Sci. **30**, 1-24.

Fricke, H. and Hart, E.J. 1966, **Chemical dosimetry.** in **Radiation Dosimetry**, vol. 2., 2nd ed., 167-239, (Attix F.H., Roesch W.C., and Tochilin E., eds.) Academic Press, New York, New York.

Fricke, H. and Morse, S., 1927, **The chemical action of roentgen rays on dilute ferrous sulfate solutions as a measure of dose**, Am. J. Roentgenol. Radium Therapy Nucl. Med. **18**, 430-432.

Fricke, H. and Petersen, B.W., 1927, **The relation of chemical, colloidal, and biological effects of roentgen rays of different wavelengths to the ionization which they produce in air. I - Action of roentgen rays on solutions of oxy-hemoglobin in water**, Am. J. Roentgenol. Radium Therapy Nucl. Med. **17**, 611-620.

Fukushima, E. and Roeder, S.B.W., 1981, **Experimental Pulse NMR**, Addison Wesley, Reading, Massachussetts.

Genser, E.E., 1962, Ph.D Thesis, University of California; cited in Hertz (1973)

Glasel, J.A., 1972, **Nuclear magnetic resonance studies on water and ice**. in **Water: A Comprehensive Treatise**, vol. 1, 215-254, (Franks, F. ed), Plenum Press, New York, New York.

Gore, J.C., Kang, Y.S., and Schulz, R.J., 1984, **Measurement of radiation dose distributions by nuclear magnetic resonance**, Phys. Med. Biol. **29**, 1189-1197.

Gore, J.C., Kang, Y.S., and Schulz, R.J, 1984b, **Measurement of radiation dose distributions by NMR imaging**, Magn. Reson. Imaging **2**, 244 (abstract).

Hart, E.J., 1955, **Radiation chemistry of the aqueous formic acid-ferric sulfate system**, J. Amer. Chem. Soc. **77**, 5786-5788.

Hart, E.J. and Matheson, M.S., 1952, **Mechanism and rate constants of the γ-ray induced decomposition of hydrogen peroxide in aqueous solutions**, Discussions Faraday Soc. **12**, 169-188.

Hart, E.J. and Platzman, R.L., 1961, **Radiation chemistry**. in **Mechanisms in Radiobiology**, vol. 1, (Errera, M. and Forssberg, A., eds.), Academic Press, New York, New York.

Hausser, R. and Noack, F., 1965, **Kernmagnetische messungen von selbstdiffusions-koeffizienten in wasser und benzol bis zum kritischen punkt**, Z. Naturforsch. **21a**, 1410-1415; cited in Glasel (1972).

Hertz, H.G., 1973, **Nuclear magnetic relaxation spectroscopy**. in **Water: A Comprehensive Treatise**, (Franks, F., ed.), vol. 3, 301-401, Plenum Press, New York, New York.

Hiraoka, T., Fukuda, H., Ikehira, A. et. al., 1986, **Digital imaging of dose distributions by magnetic resonance**, Nippon Igaku Hoshasen Gakkai Zasshi **46**, 503-505.

Horvath, A.L., 1985, **Handbook of Aqueous Electrolyte Solutions**, Wiley, New York, New York.

Huffmann, R.E. and Davidson, N., 1956, **Kinetics of the ferrous iron-oxygen reaction in sulfuric acid solutions**, J. Am. Chem. Soc. **78**, 4836-4842.

ICRU 1961, International Commission on Radiobiological Units and Measurements, Natl. Bur. Std. (US), Handbook **78**.

ICRU 1972, **Measurements of Low-Level Radioactivity**, Report **22**.

ICRU 1976, **Determination of absorbed dose in a patient irradiated by beams of x or gamma rays in radiotherapy procedures**, Report **24**.

Jayson, G.G. and Wilbraham, A.C., 1968, **The utilization of the Fricke dosimeter for evaluating the biological radiation-protective potential of water soluble organic compounds**, Chem. Commun, 641-642.

Johns, H.E. and Cunningham, J.R., 1983, **The Physics of Radiology**, 4th ed., Charles C. Thomas, Springfield, Illinois.

Koenig, S.H. and Brown, R.D., 1984, **Relaxation of solvent protons by paramagnetic ions and its dependence on magnetic field and chemical environment: implications for NMR imaging**, Magn. Reson. Med. **1**, 478-495.

Koenig, S.H. and Epstein, M., 1975, **Ambiguities in the interpretation of proton magnetic relaxation data in water solutions of Gd^{3+} ions**, J. Chem. Phys. **63**, 2279-2284.

Krenz and Dewhurst, H.A., 1949, **The mechanism of oxidation of ferrous sulfate by γ-rays in aerated water**, J. Chem. Phys. **17**, 1337.

Marcus, Y., 1983, **Ionic radii in aqueous solutions**, J. Soln. Chem. **12**(4), 271-275.

Marcus, Y., 1985, **Ionic Solvation**, Wiley, Chichester, England.

Mattsson, L.O., Johansson, K-A., and Svensson, H., 1982, **Ferrous sulfate dosimeter for control of ionization chamber dosimetry of electron and Co-60 gamma beams**, Acta Radiol. Oncol. **21**, 139-144.

Miller, N., 1953, **Chemical dosimetry at high dose rates**, Nature **171**, 688-690.

Mosse, D., Cance, K., Steinschaden, M., Chartier, A., Ostrowsky, A., and Simoen, J.P., 1982, **Determination of the yield of a ferrous sulfate dosemeter in a 35 MeV electron beam**, Phys. Med. Biol. **27**, 583-596.

Olsson, L.E., Petersson, S., Ahlgren, L., and Mattsson, S. 1988, **Measurement of Radiation Absorbed Dose With Ferrous Sulfate Solution and NMR Technique**, Internal report RADPHYS 88:02.

Olsson, L.E., Petersson, S., Ahlgren, L., and Mattsson, S., 1989, **Ferrous sulfate gels for determination of absorbed dose distributions using MRI technique: basic studies,** Phys. Med. Biol. **34**, 43-52.

Peemoeller, H. 1980, **Resolution of a Heterogeneous System NMR Response By Two Dimensional Time Evolution,** Ph.D. Thesis, University of Waterloo, unpublished.

Pfeiffer, H., 1962, **Photonenrelaxation und hydration in wassrigen losungen,** Z. Naturforsch. 17a, 279-287; cited in Koenig and Brown (1984).

Ross, C.K., Klassen, N.V., Shortt, K.R., and Smith, G.D., 1989, **A direct comparison of water calorimetry and Fricke dosimetry,** Phys. Med. Biol. **34**, 23-42.

Scharf, K. and Lee, M., 1962, **Investigation of the spectrophotometric method of measuring the ferric ion yield in the ferrous sulfate dosimeter,** Radiation Res. **16**, 115-123.

Schreiner, L.J. 1978; **Muscle Molecular Dynamics by NMR,** M.Sc thesis, University of Waterloo, unpublished.

Schreiner, L.J., MacTavish, J.C., Pintar, M.M., and Rupprecht, A., 1989, **NMR spin-grouping and correlation exchange analysis: application to low hydration NaDNA paracrystals,** accepted for publication in Biophys. J.

Schreiner, L.J. and Podgorsak, M.B., 1989, **Limits for the application of the Zimmerman-Brittin fast exchange equation in NMR relaxometry,** submitted to J. Magn. Reson.

Schulz, R.J., 1989, (private communication).

Scielzo, G., Landoni, L., and Parietti, E., 1986, **Evaluation of dose distribution in radiotherapy with magnetic resonance imaging,** Phys. Env. Biomed. Res., 403-406; cited in Olsson et al., 1988.

Shalek, R.J. and Smith C.E., 1969, **Chemical dosimetry for the measurement of high energy photons and electrons**, Ann. NY Acad. Sci. **161**, 44-62.

Simoen, J.P., 1978, in **National and International Standardization of Radiation Dosimetry**, vol. 1, Vienna, Austria.

Slichter, C.P., 1978, **Principles of Magnetic Resonance**, 2nd ed., Springer-Verlag, Berlin, West Germany.

Solomon, I., 1955, **Relaxation processes in a system of two spins**, Phys. Rev. **99**, 559-565.

Spinks, J.W.T. and Woods, R.J., 1964, **An Introduction to Radiation Chemistry**, Wiley, New York, New York.

Swift T.J. and Connick, R.E., 1962, **NMR-relaxation measurements of O^{17} in aqueous solutions of paramagnetic cations and the lifetime of water molecules in the first coordination sphere**, J. Chem. Phys. **37**, 307-320.

Szeredi, T., Leung, P.M.K., and Henkelman, R.M., 1986, **Nuclear magnetic resonance imaging in radiation dosimetry mapping**, Unpublished data.

Weiss, J., 1952, **Chemical dosimetry using ferrous and ceric sulfates**, Nucleonics **10**, No. 7, 28-31.

Zimmerman, J.R. and Brittin, W.E., 1957, **Nuclear magnetic resonance studies in multiple phase systems: lifetime of a water molecule in an adsorbing phase on silica gel**, J. Phys. Chem. **61**, 1328-1333.